Exosomal miR-205-5p enhances angiogenesis and nasopharyngeal carcinoma metastasis by targeting *desmocollin-2*

Wenjuan Yang,[1,4] Shiming Tan,[1] Lixia Yang,[1] Xiaohui Chen,[1,2] Ruiqian Yang,[1,2] Linda Oyang,[1] Jinguan Lin,[1] Longzheng Xia,[1] Nayiyuan Wu,[1] Yaqian Han,[1] Yanyan Tang,[1] Min Su,[1] Xia Luo,[1] Yiqing Yang,[1] Lisheng Huang,[1] Zifan Hu,[1] Yi Tao,[1] Lin Liu,[1] Yi Jin,[1] Hui Wang,[1,3] Qianjin Liao,[1,3] and Yujuan Zhou[1,3]

[1]Hunan Key Laboratory of Cancer Metabolism, Hunan Cancer Hospital and the Affiliated Cancer Hospital of Xiangya School of Medicine, Central South University, 283 Tongzipo Road, Changsha 410013, Hunan, China; [2]University of South China, West Changsheng Road, Hengyang 421001, Hunan, China; [3]Hunan Key Laboratory of Translational Radiation Oncology, 283 Tongzipo Road, Changsha 410013, Hunan, China

The aim of this study was to investigate whether and how exosomal miR-205-5p regulated angiogenesis and nasopharyngeal carcinoma (NPC) metastasis. We found that up-regulated serum exosomal miR-205-5p levels were associated with NPC progression and worse overall survival of NPC patients. miR-205-5p overexpression significantly increased tube formation, wound healing, migration and invasion of NPC cells, and lung metastasis of NPC tumors, whereas miR-205-5p inhibition had opposite effects. Exosomal miR-205-5p from NPC cells promoted the migration, tube formation, and microvessel density (MVD) of HUVECs *in vitro* and *in vivo*. Furthermore, bioinformatics-, luciferase reporter-, and biotinylated miR-205-5p-based pull-down assays indicated that miR-205-5p directly bound to the 3′ UTR of *desmocollin-2* (*DSC2*). Exosomal miR-205-5p targeted *DSC2* to enhance the EGFR/ERK signaling and MMP2/MMP9 expression, promoting angiogenesis and NPC metastasis, which was abrogated by DSC2 over-expression. Finally, the levels of miR-205-5p transcripts were positively correlated with MVD but negatively with DSC2 expression in NPC tissues, and patients with miR-205[high]/DSC2^{low} NPC had worse overall survival. In conclusion, exosomal miR-205-5p promotes angiogenesis and NPC metastasis by targeting DSC2 to enhance EGFR/ERK signaling and MMP expression. This exosomal/miR-205-5p/EGFR/ERK axis may be a new therapeutic target for intervention of NPC metastasis.

INTRODUCTION

Nasopharyngeal carcinoma (NPC) is one of the common head and neck malignancies in Southeast Asia, particularly in China.[1] The lymphatic and distant metastases of NPC remain a major bottleneck for survival of NPC patients.[2] Thus, revealing the molecular mechanisms underlying distant metastasis of NPC is of high significance in the clinical treatment of NPC.

Angiogenesis is crucial for tumor metastasis.[3,4] Although targeted therapies, including inhibition of angiogenesis, can slow tumor growth, there is no specific method to inhibit angiogenesis in the met-

astatic niche, preventing tumor metastasis.[5] Therefore, elucidating the molecular mechanisms by which angiogenesis mediates distant metastasis may help prevent tumor metastasis.

MicroRNAs (miRNAs) are a kind of small non-coding RNA and can regulate various biological processes by suppressing their targeted mRNA translation.[6,7] Previous studies have shown that miR-126-5p can protect the integrity of blood vessels and reduce the extent of atherosclerosis by targeting caspase-3,[8] and the miR18a/19a-TSP-1 axis can promote angiogenesis in diabetic wounds.[9] Furthermore, miRNAs can regulate the remodeling of the tumor vascular microenvironment and actuating tumor growth.[10] For example, miR-9 targets the PHD3-mediated HIF-1α/VEGF signaling to promote the development and angiogenesis of glioma,[11] while miR-182-5p inhibits colon cancer angiogenesis by targeting VEGF-C to attenuate ERK and AKT signaling.[12] Hence, different miRNAs have various functions through different targets to regulate the metastasis of cancers.

It is notable that miRNAs can be detected in extracellular vesicles, as the main source in the circulatory system.[13] Exosomes are small

extracellular vesicles of 40–160 nm in diameter and carry biological molecules of proteins, miRNA, and DNA.[14] Exosomes have excellent stability and biocompatibility and can work as effectively delivery vehicles.[15] Interestingly, exosomal miRNAs from tumor cells can paracrine-modulate non-tumor cells in the tumor microenvironment (TME) and create a pre-metastatic niche to promote distant cancer metastasis.[16,17] Among them, exosomal miR-22-3p secreted by breast cancer cells can induce abnormal tumor vessels by targeting *transgelin*, which promotes tumor budding and metastasis.[18] Exosomal miR-NAs from cancers can also be delivered to vein endothelial cells and regulate angiogenesis. For example, exosomal miR-25-3p from colorectal cancer cells can induce vascular permeability and angiogenesis in human umbilical vein endothelial cells (HUVECs) to create pre-metastatic niches.[19] In addition, exosomal miR-23a can promote angiogenesis in NPC, whereas exosomal miR-9 inhibits angiogenesis in NPC.[20,21] Moreover, miR-205 has opposite effects on different types of tumors. miR-205 can act as a tumor suppressor in skin cancer, breast cancer, and gastric cancer by targeting *TNFAIP8*, *CDK14*, and *HOXD9*.[22–25] However, miR-205 can promote tumor progression in esophageal cancer, lung cancer, ovarian cancer, and NPC by target *PTEN* and *AXIN*.[26–30] Evidently, miR-205-5p is highly expressed in NPC and can promote the development and progression of NPC,[29,31] but the role of exosomal miR-205-5p in the metastasis of NPC has not been clarified.

In this study, we found that miR-205-5p was associated with distant metastasis of NPC. More important, exosomal miR-205-5p from NPC cells induced angiogenesis of HUVECs, which facilitated NPC metastasis by targeting *DSC2* to enhance the EGFR and ERK signaling. Our findings may uncover novel molecular mechanisms by which exosomal miR-205-5p induces NPC angiogenesis and promotes its metastasis and reveal new therapeutic targets for intervention of NPC.

RESULTS

Up-regulated miR-205-5p transcripts are positively associated with distant metastasis and poor prognosis of NPC

A previous report has shown that miR-205-5p expression increases in cisplatin-resistant NPC HNE1 cells.[31] To view miR-205-5p expression in NPC, we analyzed the relative levels of miR-205-5p transcripts in control NP69 and NPC CNE1, CNE2, HNE2, and 5-8F cells using quantitative real-time PCR. Compared with NP69, the relative levels of miR-205-5p transcripts in NPC cells significantly increased (Figure S1A). A similar pattern of the levels of miR-205-5p transcripts was observed in the supernatants of cultured cells (Figure S2A).

Next, we screened the NPC-related differentially expressed genes (DEGs) in the GEO database (GEO: GSE22587 and GEO: GSE43039) and found that the levels of miR-205 transcripts in NPC tissues were significantly higher than non-tumor tissues or inflamed tissues (p < 0.05 and p < 0.001; Figures S1B and S1C). *In situ* hybridization (ISH) analysis of miR-205-5p transcripts in 135 NPC specimens revealed that the levels of miR-205-5p transcripts in stage III and IV NPC specimens (n = 112) were significantly higher

than in stage I and II NPC specimens (n = 23) (p < 0.001; Figures S1D and S1E). Moreover, the levels of miR-205-5p transcripts in distant metastatic NPC specimens (n = 116) were significantly higher than in NPC specimens without distant metastasis (n = 19) (p < 0.001; Figures S1F and S1G). More important, high levels of miR-205-5p transcripts were related to shorter overall survival of 75 NPC patients (p < 0.05; Figure S1H; Table S1). Together, up-regulated miR-205-5p transcripts were associated with higher tumor stages, distant metastasis, and worse prognosis of NPC.

MiR-205-5p enhances metastatic behaviors of NPC cells

Given that higher levels of miR-205-5p transcripts were detected in CNE1, HEN2, and 5-8F cells, we selected them for subsequent experiments. To test the function of miR-205-5p in metastatic behaviors of NPC cells, we transfected CNE1, HNE2, and 5-8F cells with miR-205-5p mimic and miR-205-5p inhibitor. The quantitative real-time PCR results indicated that compared with the control (miR-NC) group, transfection with the miR-205-5p mimic significantly increased, while transfection with the miR-205-5p inhibitor dramatically decreased the relative levels of miR-205-5p transcripts in NPC cells by about 75%, showing miR-205-5p over-expression and silencing, respectively (p < 0.01 and p < 0.001; Figure S2B).

Functional analyses exhibited that although miR-205-5p over-expression significantly increased the number of tubes, wound healing, migrated and invaded CNE1, HNE2, and 5-8F cells, miR-205-5p silencing significantly decreased the number of tubes, wound healing, migrated and invaded CNE1, HNE2, and 5-8F cells (p < 0.05, p < 0.01, and p < 0.001; Figures S2C, S2D, S3A, and S3B). These data clearly demonstrated that miR-205-5p acted as an oncogenic factor to promote the wound healing, migration, invasion, and vasculogenic mimicry (VM) of NPC cells. Moreover, compared with the control, intravenous injection with miR-205-5p over-expressing 5-8F cells significantly increased the numbers of lung metastatic NPC nodules, while injection with miR-205-5p-silencing 5-8F cells significantly decreased the numbers of lung metastatic nodules in nude mice (p < 0.05 for all; Figure S3C). Collectively, miR-205-5p acted as an oncogenic factor to promote metastatic behaviors of NPC cells *in vitro* and *in vivo*.

High levels of exosomal miR-205-5p are related to the progression of NPC

To explore the function of exosomal miR-205-5p in the progression of NPC, we analyzed miRNAs in 3 serum exosomal samples from NPC patients and 3 from non-tumor human subjects by miRNA sequencing. We found 1,087 differentially expressed miRNAs between the serum exosomes of NPC patients and non-tumor subjects. Next, we screened 29 miRNAs with significantly different levels ($\log_2$ (fold change) > 2 or $\log_2$ (fold change) < −2), and after removed un-named genes, we found the miR-205-5p was the most up-regulated in serum exosomes from NPC patients (Figures 1A–1C). Further quantitative real-time PCR exhibited that the levels of miR-205-5p transcripts in 88 NPC serum exosomal samples were significantly higher than in 6 healthy subjects (p < 0.001; Figure 1D). Moreover, higher
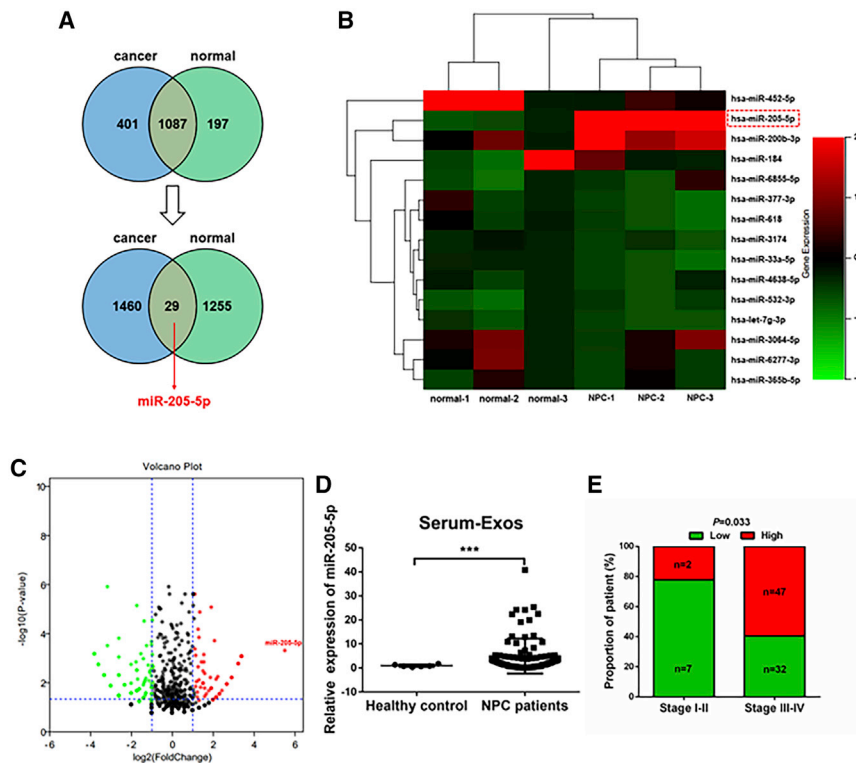
Figure 1. High levels of serum exosomal miR-205-5p are associated with the progression of NPC

(A) Identification of differentially expressed miRNAs by sequencing of 3 serum samples from NPC patients and 3 serum samples from healthy subjects. The Venn diagram indicates 29 miRNAs with more significant differences among 1,087 differentially expressed miRNAs. There were 401 miRNAs expressed only in the serum exosomes from NPC patients and 197 miRNAs expressed only in the serum exosomes from non-tumor subjects. There were 1,460 miRNAs expressed only in the serum exosomes of NPC patients, but with no significant difference ($\log_2$ (fold change) < 2 or $\log_2$ (fold change) > −2), and 1,255 miRNAs expressed only in the serum exosomes of non-tumor subjects with no significant difference ($\log_2$ (fold change) < 2 or $\log_2$ (fold change) > −2). (B) Heatmap analysis of 15 miRNAs. Red, up-regulated miRNAs; green, down-regulated miRNAs. The solid red box highlights the up-regulated miR-205-5p in NPC patients. (C) A volcano plot displayed the distribution of differentially expressed miRNAs. (D and E) High levels of serum exosomal miR-205-5p transcripts were related to higher stages of NPC in this population. The levels of serum miR-205-5p transcripts in individual patients (n = 88) and healthy subjects (n = 6) were determined using quantitative real-time PCR. ***p < 0.001.

levels of serum exosomal miR-205-5p transcripts were associated significantly with higher clinical stages of NPC in this population (p = 0.033; Figure 1E). Hence, higher levels of serum exosomal miR-205-5p transcripts were related to the progression of NPC.

Exosomal miR-205-5p from NPC cells fuses to HUVECs

Intracellular miRNAs can be carried and secreted through exosomes to participate in the communication between different cells.[32] Accordingly, we explored whether exosomes from NPC cells could deliver miR-205-5p to HUVECs. We isolated exosomes from the serum samples of non-tumor subjects and NPC patients or from the supernatants of cultured NP69 and 5-8F cells. Transmission electron microscopy (TEM) and NanoSight particle tracking analyses displayed an exosome teacup-like double-sided structure of 40–160 nm (Figures 2A and 2B). In addition, western blotting demonstrated the presence of HSP70, TSG101, the specific endosomal markers, and CD63, the surface marker, in the purified exosomes from the conditioned medium and serum (Figure 2C). Moreover, confocal microscopy showed that treatment of HUVECs with (4′,6-diamidino-2-phenylindole, blue) and PKH67 (green)-labeled exosomes for 24 h promoted their fusion with an intracytoplasmic punctuating green fluorescent signal in HU-VECs (Figure 2D).

Exosomal miR-205-5p induces angiogenesis *in vitro* and *in vivo*

To determine the impact of exosomal miR-205-5p on angiogenesis, we explored how exosomal miR-205-5p affected the migration and tube formation of HUVECs. We collected exosomes from miR-205-5p

over-expressing and silencing NPC cells as miR-205-5p mimic-exo and miR-205-5p inhibitor-exo, respectively. We treated HUVECs with 10 μg of each type of exosomes for 48 h.[33] We found that compared with that in the controls, treatment with miR-205-5p mimic-exo from CNE1, HNE2, and 5-8F cells significantly increased the relative levels of miR-205-5p transcripts, while treatment with miR-205-5p inhibitor-exo from the same cells remarkably decreased miR-205-5p transcripts in HUVECs (p < 0.001 for all; Figure S4A). Furthermore, miR-205-5p mimic-exo from CNE1, HNE2, and 5-8F cells significantly enhanced the migration and tube formation of HUVECs, whereas miR-205-5p inhibitor-exo from the same cells had opposite effects on HUVECs (p < 0.01 and p < 0.001; Figures 3A, 3B, and S4D–S4F). Similarly, transfection with miR-205-5p mimic also enhanced the migration and tube formation, whereas transfection with miR-205-5p inhibitor reduced the migration and tube formation in HUVECs (Figures S4G–S4J). *In vivo* Matrigel plug assays exhibited that treatment with miR-205-5p mimic resulted in obvious blood vessel traces on the surface of gel plugs, while treatment with miR-205-5p inhibitor-exon did not induce obvious blood vessel traces on the surface of gel plugs (Figure 3C). HE staining displayed a denser microvessel structure in the miR-205-5p mimic-treated HUVECs but only a looser microvascular structure in the miR-205-5p inhibitor-treated cells (Figure 3D). Quantitative analyses revealed that microvessel density (MVD) in the miR-205-5p mimic-treated HUVECs was significantly higher than in the control, whereas MVD in the miR-25-5p inhibitor-treated HUVECs was less than that of the control (Figure 3D). Therefore, exosomal miR-205-5p from NPC cells promoted angiogenesis *in vivo* and *in vitro*.
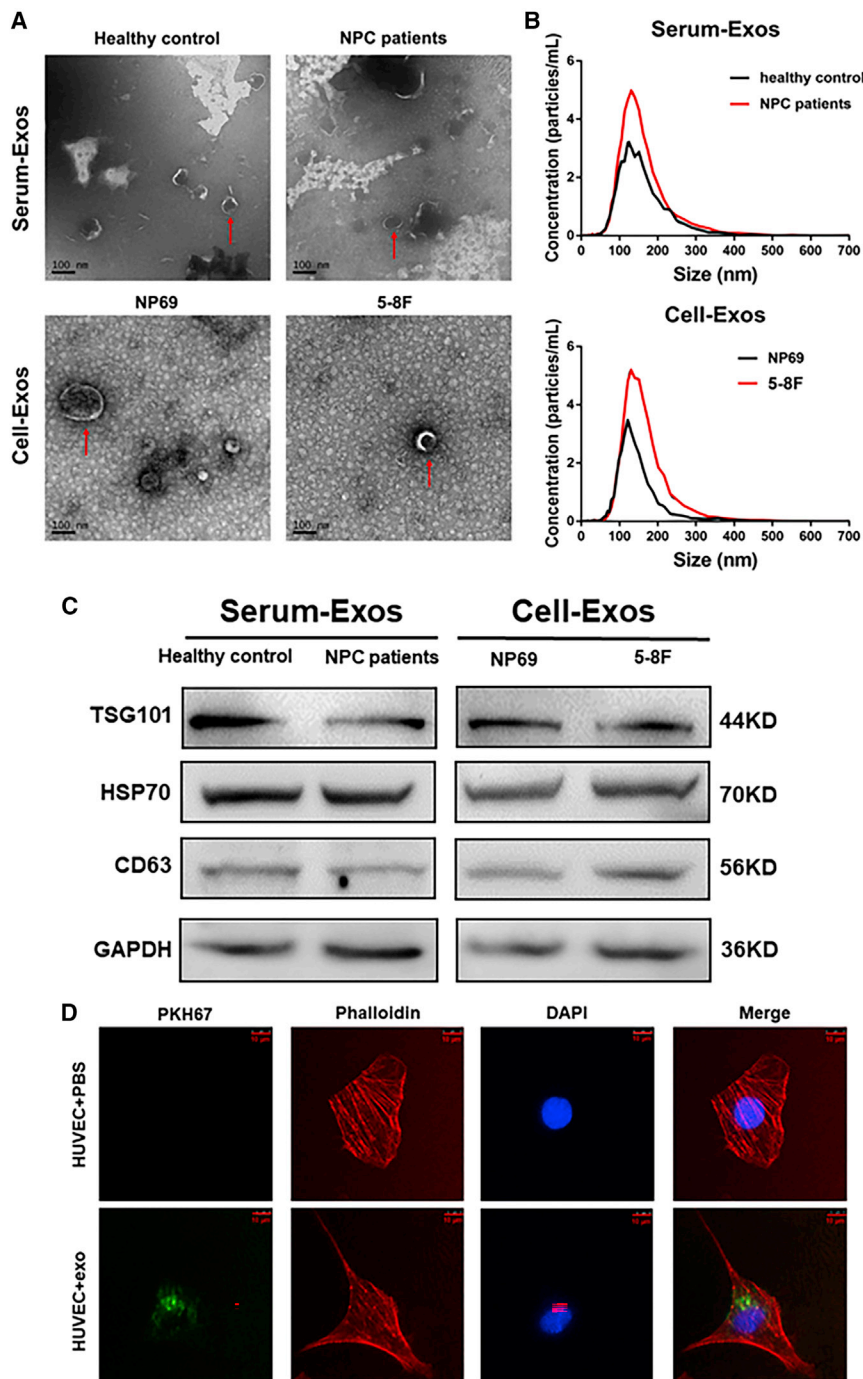
Figure 2. NPC-secreted exosomes enter into HUVECs

(A) Characterization of exosomes from NPC patient and healthy subject sera or from NP69 and 5-8F cells by transmission electron microscopy. Red arrows highlight exosomes. Scale bar, 100 nm. (B) Nanoparticle tracking analysis of the size distribution of exosomes isolated from sera and cells. (C) Western blot analysis of the expression of the indicated molecules in serum and cell exosomes. (D) Fluorescent imaging analysis of exosomes entering into HUVECs. HUVECs were treated with control PBS or 5-8F exosomes that had been labeled with PKH67 (green) for 24 h and stained with phalloidin (red) and DAPI (blue) for confocal microscopy analysis. Scale bar, 10 μm.

and migration of tumor cells.[34] Bioinformatics predicted that the 3′ UTR of *DSC2* mRNA contained the miR-205-5p binding sites (Figure 4A). To test the function of miR-205-5p and exosomal miR-205-5p, we cloned the 3′ UTR (wild-type [WT] 3′ UTR) of *DSC2* and its mutant (mut 3′ UTR) into the luciferase reporter vector. Dual luciferase reporter assays indicated that transfection with miR-205-5p or exosomal miR-205-5p, together with GV238-DSC2-3′ UTR-WT, significantly reduced the luciferase activities in 5-8F cells and HUVECs (p < 0.01 and p < 0.001; Figures 4B and 4C). In contrast, transfection with miR-205-5p or exosomal miR-205-5p and GV238-DSC2-3′ UTR-mut did not significantly change the luciferase activity in 5-8F cells and HUVECs. In addition, a biotinylated miR-205-5p pull-down assay was applied to examine whether miR-205-5p and exosomal miR-205-5p could directly interact with *DSC2* mRNA in NPC cells. The results indicated that the levels of DSC2 mRNA by biotinylated or exosomal miR-205-5p markedly increased compared with the negative control (p < 0.05; Figure 4D). These independent lines of evidence demonstrated that miR-205-5p directly bound to the 3′ UTR of *DSC2* mRNA to inhibit its expression.

To further investigate the molecular mechanisms underlying the action of exosomal miR-205-5p in inducing angiogenesis and promoting NPC

Exosomal miR-205-5p targets *DSC2* to attenuate the EGFR and ERK signaling in NPC cells

To understand the mechanisms underlying the actions of exosomal miR-205-5p in angiogenesis and metastasis of NPC, we used TargetScan and miRBase to predict many potential genes the miR-205-5p targeted. It was notable that *DSC2*, a tumor suppressor, was one potentially targeted gene that had been shown to inhibit the invasion

metastasis, we examined EGFR and ERK signaling, given that they are crucial for tumor angiogenesis.[20,35] Western blot showed that transfection with miR-205-5p mimic significantly reduced the relative levels of DSC2 protein expression but enhanced EGFR and ERK1/2 phosphorylation in CNE1, 5-8F, and HNE2 cells, while transfection with miR-205-5p inhibitor increased DSC2 expression but decreased EGFR and ERK1/2 phosphorylation in these cells (Figures 4E and

detected in the miR-205-5p-overexpressed CNE1, HNE2, and 5-8F cells that had been transfected with the control vector (Figures 5A, S5A–S5C, and S6A–S6C). In contrast, induction of DSC2 over-expression significantly decreased tube formation, migration, and invasion in the control cells and almost completely abrogated miR-205-5p-enhanced tube formation, migration, and invasion in the miR-205-5p-overexpressed CNE1, HEN2, and 5-8F cells. A similar pattern of migration and tube formation was observed in the different groups of HUVECs following transfection with miR-205-5p and induction of DSC2 over-expression (Figures 5B and 5C).

Metal matrix metalloproteinase (MMP) can promote tumor metastasis and angiogenesis by degrading extracellular matrix proteins. MMP2 and MMP9, two members of the MMP family, are crucial for tumor metastasis, VM, and angiogenesis, and their expression is positively regulated by activated ERK.[36–38] Western blot analysis revealed that compared with the control group (miR-NC + DSC2-vector or miR-NC-exo + DSC2-vector), induction of DSC2 over-expression not only decreased the relative levels of EGFR and ERK phosphorylation but also down-regulated MMP2 and MMP9 expression in NPC cells and HUVECs (Figures 5D, 5E, and S7B). More important, induction of DSC2 over-expression almost completely abrogated miR-205-5p mimic- and miR-205-5p mimic-exo-enhanced EGFR and ERK phosphorylation as well as MMP2 and MMP9 expression in NPC cells and HUVECs (Figures 5D, 5E, and S7B). Therefore, DSC2 over-expression abrogated the enhancement of exosomal miR-205-5p in angiogenesis and metastatic behaviors of NPC cells and HUVECs.

S7A). Similarly, treatment with miR-205-5p mimic-exo from 5-8F cells also remarkably decreased DSC2 expression but increased EGFR and ERK1/2 phosphorylation, while treatment with miR-205-5p inhibitor-exo from 5-8F cells up-regulated DSC2 expression but down-regulated EGFR and ERK1/2 phosphorylation in HUVECs (Figure 4F). Thus, exosomal miR-205-5p targeted DSC2 to attenuate the EGFR and ERK signaling in NPC cells and HUVECs.

DSC2 over-expression eliminates angiogenesis and metastasis induced by exosomal miR-205-5p

To confirm that exosomal miR-205-5p targeted *DSC2* to enhance angiogenesis and NPC metastasis, we transfected miR-205-5p-overexpressed CNE1, HNE2, and 5-8F cells with a plasmid for DSC2 expression or control vector. Compared with that in the miR-NC-transfected control cells, significantly increased VM, migration, and invasion were
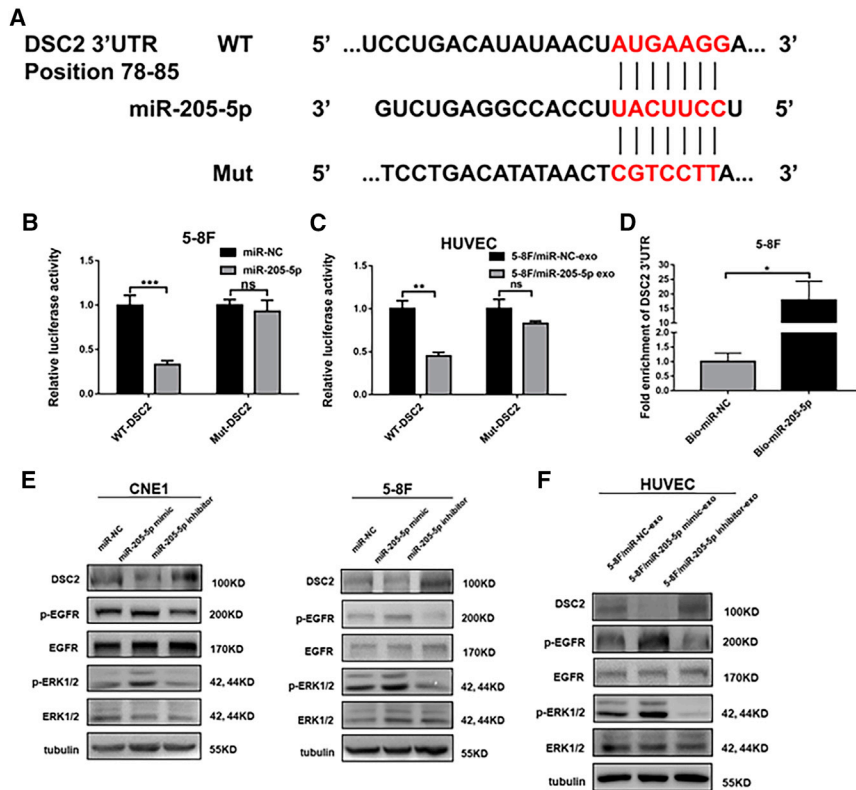
Figure 4. MiR-205-5p targets *DSC2* to enhance the EGFR and ERK signaling in NPC cells and HUVECs

(A) Schematic illustration of the predicted binding sequence in the 3′ UTR of *DSC2* and its mutant. (B and C) Luciferase reporter assays revealed that miR-205-5p over-expression or exosomal miR-205-5p significantly reduced the DSC2-3′ UTR but not its mutant-regulated luciferase expression in 5-8F cells and HUVECs. (D) Quantitative real-time PCR analysis of the levels of *DSC2* mRNA 3′ UTR in the strepta-vidin beads pulled-down from the lysates of cultured 5-8F cells that had been transfected with the control or biotinylated miR-205-5p. (E) Western blot analysis of the relative levels of DSC2, EGFR, and ERK1/2 expression and EGFR and ERK1/2 phosphorylation in NPC cells after transfection with miR-NC, miR-205-5p mimic and miR-205-5p inhibitor, respectively. (F) Western blot analysis of the relative levels of DSC2, EGFR, and ERK1/2 expression and EGFR and ERK1/2 phosphorylation in HUVECs after treatment with the indicated types of exosomes. Data are representative images or expressed as mean ± SD of each group from three separate experiments. **p < 0.01 and ***p < 0.001.

Cell culture and treatment

Human NPC CNE1, CNE2, HNE2, and 5-8F, immortalized nasopharyngeal epithelial non-tumor NP69, and human umbilical vein endothelial cells were obtained from the Cancer Institute of Central South University and identified by STR. The cells were cultured in RPMI-1640 medium containing 10% fetal bovine serum (FBS), 100 U/mL penicillin, and 100 μg/mL streptomycin (Biological Industries, Beit Haemek, Israel) in a 5% CO_2 incubator.

The levels of miR-205-5p transcripts are correlated positively with MVD but negatively with DSC2 expression in NPC

To look for clinical relevance of miR-205-5p transcripts, we evaluated the potential relationship among the levels of miR-205-5p transcripts, DSC2 expression, and MVD in NPC tissue samples. We found that high levels of miR-205-5p transcripts were accompanied by higher MVD but lower DSC2 expression in NPC tissues (Figures 6A and 6B). Quantitative analyses indicated the levels of miR-205-5p transcripts were correlated positively with MVD (p < 0.001) but negatively with DSC2 expression (p < 0.001), while MVD was also negatively correlated with DSC2 expression in NPC tissues (p < 0.001; Figures 6C–6E). To understand the value of miR-205-5p and DSC2 expression, we stratified 75 NPC patients into higher miR-205-5p/lower DSC2, lower miR-205-5p/higher DSC2, and another group (higher miR-205-5p/higher DSC2 and lower miR-205-5p/lower DSC2), according to the levels of miR-205-5p transcripts and DSC2 expression. We

found that patients with higher miR-205-5p/lower DSC2 NPC had significantly worse overall survival than those with lower miR-205-5p/higher DSC2 NPC in this population (p < 0.05; Figure 6F; Table S2). Actually, patients with higher DSC2 expressing NPC had slightly better overall survival than those with lower DSC2 expressing NPC (Figure S7C). Therefore, higher miR-205-5p transcripts were associated with increased risk for worse prognosis of NPC by targeting *DSC2*.

DISCUSSION

This study highlighted that NPC-derived exosomal miR-205-5p promoted NPC metastasis by inducing angiogenesis. Invasion and metastasis are important biological behaviors of cancer cells and can seriously threaten the life quality of cancer patients.[39–41] Therefore, exploring the molecular mechanisms by which exosomal miR-205-5p modulates the distant metastasis of NPC will be of significance for improving the survival of NPC patients. It has been shown that miR-205-5p can inhibit the proliferation and migration of skin cancer cells[22] and invasion of gastric cancer cells as well as lymph node metastasis,[24] suggesting that miR-205-5p acts as a tumor suppressor. In contrast, miR-205 promotes the proliferation and migration of lung and ovarian cancer cells by targeting *PTEN* and *SMAD4* to enhance PI3K/AKT signaling.[27,28] In this study, we found that up-regulated miR-205-5p transcripts were associated with progression and worse prognosis of NPC, consistent with previous observations.[30,31] Functionally, miR-205-5p acted as an oncogenic factor to enhance the metastatic behaviors of NPC. Collectively, these findings indicate that miR-205-5p has different functions in different types of cancers.
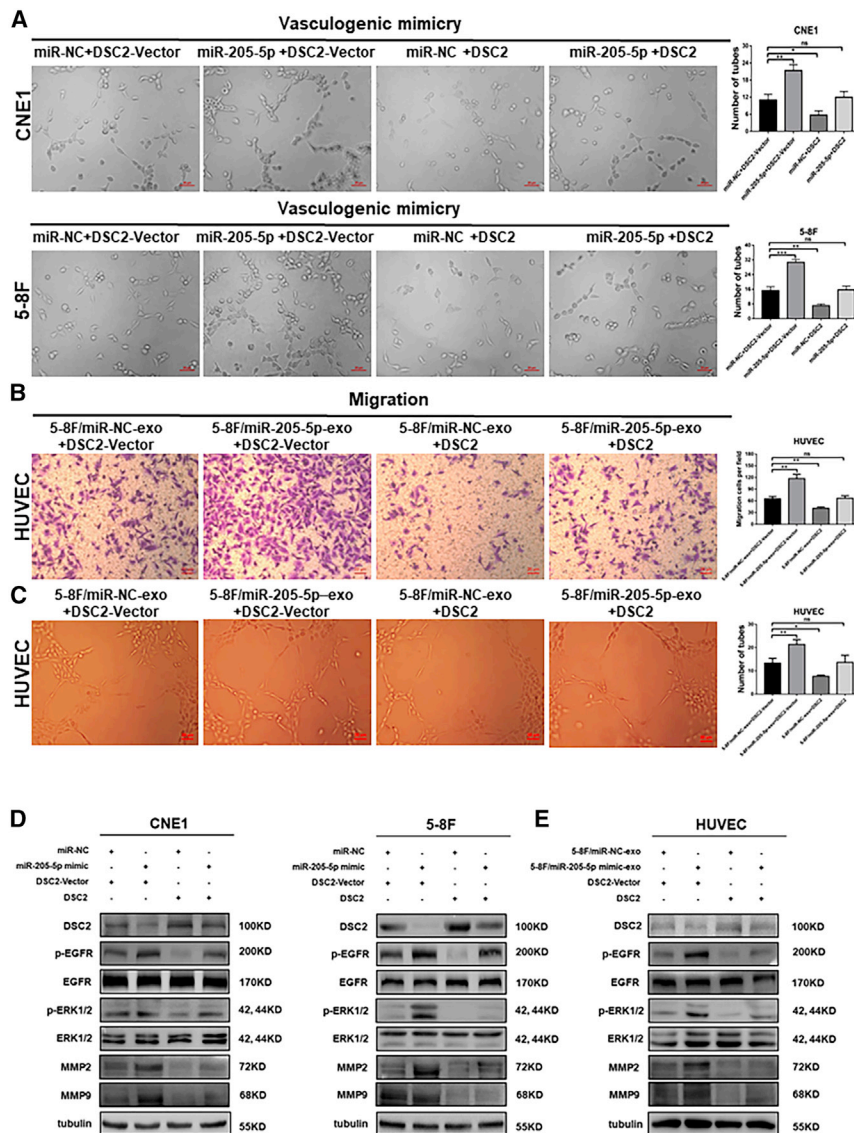
Figure 5. Induction of DSC2 over-expression abrogates the miR-205-5p-enhanced angiogenesis and metastatic behaviors of NPC cells and HUVECs

CNE1, 5-8F cells, and HUVECs were transfected with control vector, plasmid for DSC2 expression, together with control miR-NC or miR-205-5p or treatment with exosomes from the indicated cells. The cells were tested for tube formation, migration, invasion, and the relative levels of DSC2, EGFR, ERK1/2, MMP2, and MMP9 expression as well as EGFR and ERK1/2 phosphorylation. (A) The effects of DSC2 over-expression on VM in the indicated cells. Scale bar, 20 μm. (B and C) The effects of DSC2 over-expression on the migration and tube formation of the indicated HUVECs. Scale bar, 20 μm. (D and E) Western blot analyses of the relative levels of DSC2, EGFR, ERK1/2, MMP2, and MMP9 expression and EGFR and ERK1/2 phosphorylation in the indicated cells. Data are representative images or expressed as mean ± SD of each group from three separate experiments. *p < 0.05, **p < 0.01, and ***p < 0.001.

cell angiogenesis by targeting exosomal miR-205-5p may be valuable for inhibiting the distant metastasis of NPC.

We found that *DSC2*, a tumor suppressor, was one of the genes the miR-205-5p targeted, extending previous observation of miR-205-5p targeting *PTEN*.[31] Actually, DSC2 acts as a tumor suppressor, and its deficiency is observed in malignant lesions, including skin cancer, colon cancer, and esophageal squamous cell carcinoma.[34,46–48] DSC2 can attenuate the EGFR/ERK/AKT signaling and inhibit the progression of different types of cancers.[48–50] Given that EGFR is highly expressed in metastatic NPC tissues and is enriched in extracellular vesicles from NPC cells,[51] we found that exosomal miR-205-5p targeted *DSC2* to enhance EGFR and ERK phosphorylation, MMP2 and MMP9 expression, and metastatic behaviors of NPC cells, supporting the notion that activation of the EGFR/ERK signaling can enhance MMP2 and MMP9 expression.[52–57] Such novel data indicate that DSC2 inhibits the EGFR/ERK signaling in NPC cells and angiogenesis in HUVECs, extending previous findings in other types of cancers.[49,50,53–57]

We recognized that our study had limitations. It is well known that exosomes originate from cavities or early endosomes in the circulation pathway of the plasma membrane.[58] In this study, we identified exosomes on the basis of their diameters and molecular characteristics but did not trace their germination process, so that the identified exosomes might contain other types of extracellular vesicles (EVs).[59,60] Second, tumor angiogenesis is regulated by exosomal miRNAs and other factors, such as cytokines and chemokines.[14] Our study centered on exosomal miR-205-5p, but we did not explore the potential role of

Microvessel formation and angiogenesis are critical for tumor growth and metastasis. Tumor cell-derived exosomes can regulate angiogenesis in tumors,[42] because the biologically active cargos in exosomes can be endocytosed by endothelial cells, changing the endothelial cell functions.[43] Exosomal miR-22-3p from breast cancer cells can induce tumor vessel abnormality to promote tumor budding.[18] Furthermore, exosomal miR-25-3p from colorectal cancer and exosomal miR-619-5p from lung cancer can promote angiogenesis.[19,44] Although exosomal miR-23a from NPC enhances angiogenesis, exosomal miR-9 can inhibit angiogenesis.[20,21] It is notable that exosomal miR-205-5p can target *PTEN* to induce angiogenesis in ovarian cancer.[45] In this study, we found that exosomal miR-205-5p from NPC cells promoted angiogenesis. Such novel findings indicated that exosomal miR-205-5p enhanced the angiogenesis of endothelial cells to promote the distant metastasis of NPC. Hence, control of endothelial
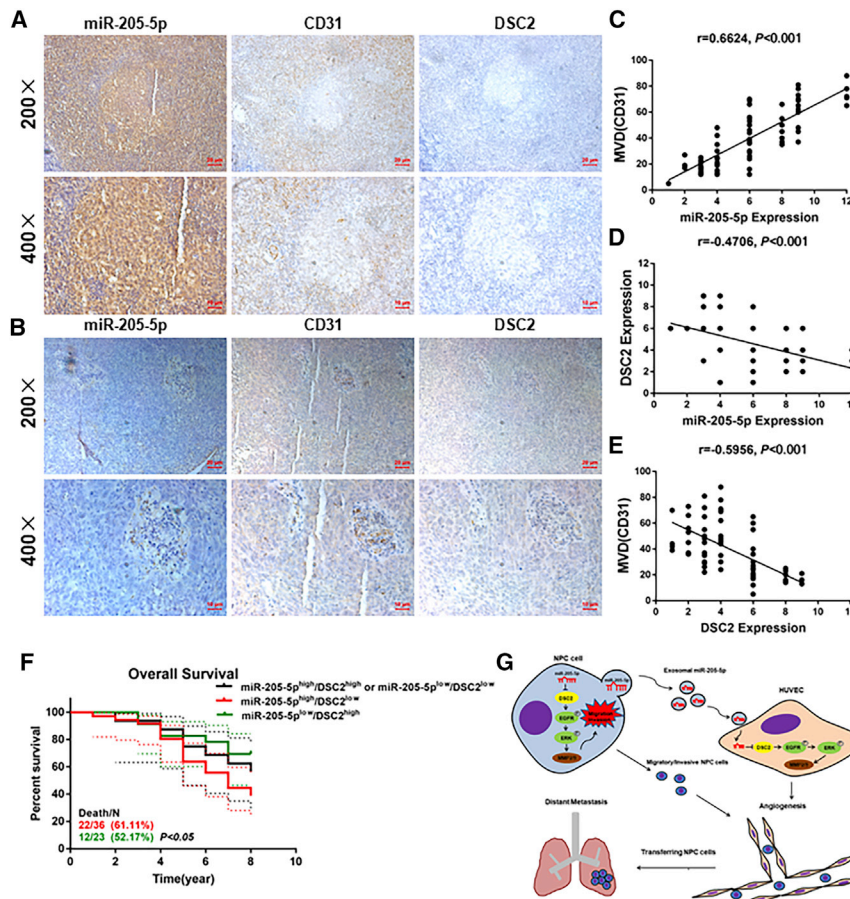
Figure 6. The levels of miR-205-5p transcripts are correlated positively with microvessel density but negatively with DSC2 expression in NPC

(A and B) IHC analysis of CD31 and DSC2 expression in NPC tissues with low or high miR-205-5p transcripts. The scale bar in 200× images represents 50 μm. The scale bar in 400× images represents 10 μm. (C–E) The correlation among the levels of miR-205-5p transcripts, DSC2 expression, and MVD in NPC tissues. (F) Stratification analysis indicated that patients with miR-205-5p^high/DSC2^low NPC had worse overall survival than other groups of patients in this population. (G) Diagram illustrating the mechanisms by which NPC-secreted exosomal miR-205-5p induced angiogenesis by targeting *DSC2* to facilitate NPC metastasis. Up-regulated serum exosomal miR-205-5p levels were associated with NPC progression. Exosomal miR-205-5p promotes angiogenesis and NPC metastasis by targeting DSC2 to enhance the EGFR/ERK signaling and MMP expression. Patients with miR-205^high/DSC2^low NPC had worse overall survival.

and horseradish peroxidase (HRP)-conjugated second antibodies, followed by development with DAB.[61] The numbers of microvessels in five fields (magnification 200×) randomly selected were counted in a blinded manner, and the levels of DSC2 expression were quantified using ImageJ software.

In situ hybridization

The levels of miR-205-5p transcripts in individual NPC tissues were quantified by ISH using the enhanced *in situ* hybridization kit (MK1030; BOSTER, China), per the manufacturer's protocol. Briefly, NPC tissue sections (4 μm) were blocked with endogenous peroxidase with 30% H_2O_2 in methanol and penetrated with pepsin. Subsequently, the sections were pre-hybridized and hybridized with a miR-205-5p specific 5′-GIG-dUTP tagged probe (5′-CAGACUCCGGUGGAAUGAAGGA-3′; Sangon Biotech, Shanghai, China). After being extensively washed, the sections were blocked, and the bound probes were detected with biotinylated anti-digoxin, followed by reaction with SABC. Finally, the sections were treated with biotinylated HRP, developed with DAB, and counterstained with hematoxylin. The distribution and intensity of probed signals were semi-quantitatively scored for signal intensity (0 = no staining, 1 = light brown, 2 = brown cells without background staining or dark brown cells with light brown background, and 4 = dark brown cells without background staining) and for the percentage of positive cells (0 = no positive cells, 1 = ≤25% positive cells, 2 = 26%–49% positive cells, 3 = 50%–74% positive cells, 4 = ≥75% positive cells). As a result, a final score was the product of the intensity and percentage scores. We stratified NPC tissues as negative staining with a final score of 0, weakly positive with a final scores of 1 or 2, moderately staining with a final score of 3 or 4, and strongly staining with a final score of more than 5.

other factors simultaneously. We are interested in further investigating whether exosomal miR-205-5p also regulates the expression and function of these factors to avoid potential misleading.

MATERIALS AND METHODS
Human tissue samples
All participants provided written informed consent. The study was approved by the Ethical Review Committee of Hunan Cancer Hospital (approval number SBQLL-2018-044). A total of 135 surgical specimens were collected from NPC patients at Hunan Cancer Hospital, and they were fixed and paraffin-embedded. Tissue sections were pathologically examined by experienced pathologists to confirm the NPC diagnosis. Among them, 75 NPC patients had completely clinical data.

Peripheral venous blood samples were obtained from 88 NPC patients and 6 healthy subjects before any antitumor therapy, and their serum samples were prepared.

Immunohistochemistry
The contents of MVD and levels of DSC2 expression in NPC tissue sections were characterized by immunohistochemistry (IHC) using anti-CD31 (1:100 dilution; ab28364; Abcam, Cambridge, MA) or anti-DSC2 (1:1,000 dilution; 13876-1-AP; Proteintech, Chicago, IL)

Isolation and identification of exosomes and treatment

Exosomes were extracted from individual serum samples of NPC patients and conditional media of cultured NPC cells by differential ultracentrifugation using an ExoQuick-TC exosome isolation kit (System Biosciences, Palo Alto, CA). Briefly, the collected serum and conditioned medium samples were sequentially centrifuged at $300 \times g$ for 10 min and $2,000 \times g$ for 10 min and mixed with ExoQuick-TC solution and centrifuged at $10,000 \times g$ for 30 min. The supernatants were filtered using a 0.22 µm filter and centrifuged at $100,000 \times g$ for 70 min (all centrifugation at 4°C). The resulting pellets were re-suspended in PBS.

The collected exosomes were placed on the copper mesh and stained with 2% uranyl acetate, followed by examination under a transmission electron microscope (G2 Spirit; FEI). Brownian motion and concentrations of exosomal samples were analyzed using ZetaView 8.04.02 SP2 (ZetaView PMX 110, Particle Metrix, Germany). Furthermore, exosomes were characterized by western blot using antibodies against HSP70 (1:500; 66183-1-Ig; Proteintech), CD63 (1:500; ab216130; Abcam), and TSG101 (1:500; ab30871; Abcam).

In addition, different groups of cells (1×10^5 cells/well) were treated with 10 µg exosomes for 48 h. Cells were analyzed in subsequent experiments. The purified exosomes were labeled with PKH67 (Sigma-Aldrich, St. Louis, MO).[33]

Transfection

CNE1 cells, HEN2 cells, 5-8F cells, and HUVECs at 70% confluency were transfected with miR-205-5p mimic, miR-205-5p inhibitor, or their scramble controls (Shanghai Sangon Biological, Shanghai, China) or plasmid for DSC2 expression or its negative control (Shanghai GeneChem, Shanghai, China) using Lipofectamine 3000 (Invitrogen, Waltham, MA). After 24 h incubation, the transfection efficiency was determined using quantitative real-time PCR.

Wound-healing assay, tube formation assay, Transwell migration, and invasion assays

Wound-healing assay, Transwell migration, and invasion assays were performed as described previously.[62] For the tube formation assay, HUVECs (5,000 cells/well) were treated with NPC cell-derived exosomes for 48 h, and the treated cells at 2×10^4 cells/well were cultured in 96-well plates that had been coated with Matrigel (50 µL/well; 356230; BD Pharmingen) for 4–8 h. The tubular structures in individual wells were photoimaged under an inverted microscope.

Matrigel plug assay

The study was approved by the Ethical Review Committee of Hunan Cancer Hospital (approval number: KYJJ-2018-019). The impact of exosomes on *in vivo* angiogenesis of HUVECs was analyzed using Matrigel plug assays. HUVECs were treated with exosomes from the different groups of 5-8F cells for 48 h as 5-8F/miR-NC-exo, 5-8F/miR-205-5p-exo, and 5-8F/anti-miR-205-5p cells. The exosome-treated HUVECs (3×10^6 cells in 500 µL) were mixed with 500 µL Matrigel. The mixtures were injected subcutaneously into BALB/c nude mice (female, 6–8 weeks old). Two weeks later, the implanted Matrigel plugs were recovered, fixed, photoimaged, sectioned, and stained with signature red and hematoxylin. The animal experimental protocols were approved by the Animal Experiment and Ethics Committee of Hunan Cancer Hospital.

In vivo tumor lung metastasis assay

The study was approved by the Ethical Review Committee of Hunan Cancer Hospital (approval number: KYJJ-2018-019). Individual BALB/c nude mice were injected intravenously (tail vein) with 2×10^6 5-8F/miR-NC, 5-8F/miR-205-5p, and 5-8F/miR-205-5p-inhibitor cells. Eight weeks later, the mice were euthanized and their lungs tissues were dissected, fixed, sectioned, and stained with H&E. The numbers of metastatic tumors were quantified in a blinded manner.

Luciferase reporter assay

The potential targeting of miR-205-5p to *DSC2* was analyzed using dual luciferase reporter assay.[22] Briefly, the 3′ UTR of *DSC2* for potential binding of miR-205-5p (wild-type) or its mutant sequence (mutant type) was cloned into GV238 vector (GeneChem) to generate GV238-DSC2-3′ UTR-WT and GV238-DSC2-3′ UTR-mut, respectively. 5-8F cells and HUVECs were transfected with GV238-DSC2-3′ UTR-WT or GV238-DSC2-3′ UTR-mut, together with miR-205-5p mimic or its negative control for 48 h. The luciferase activities in different groups of cells were analyzed using the Dual Luciferase Reporter Assay System (Promega).

Biotinylated miR-205-5p pull-down assay

The biotinylated miR-205-5p-based pull-down assay was performed as described.[63] Briefly, 5-8F cells were transfected with biotinylated miR-205-5p or scrambled control (Sangon Biotech) and collected 48 h after transfection. 5-8F cells were cross-linked with 1% glutaraldehyde and 1.25 µM glycine. The cell lysates were incubated with M-280 streptavidin magnetic beads (11205D; Invitrogen) in the presence of 10 µL of yeast tRNA (AM7119; Invitrogen) on a rotator at 4°C for 2 h. After being washed, the bound RNAs were extracted with TRIzol (Invitrogen). The contents of DSC2 mRNA 3′ UTR sequence were determined using quantitative real-time PCR. The 3′ biotinylated miR-205b-5p sequence was 5′-UCCUUCAUUCCACCGGAGUCUG-3′ BiO. The scrambled control miRNA sequence was 5′-UUUUUUCUUUUGGGUUAUUGA-3′ BiO.

Quantitative real-time PCR

We extracted total RNA from individual samples using TRIzol reagent (Invitrogen) and reversely transcribed them (1 µg each sample) or exosomal total RNAs (0.25 µg) into cDNA using cDNA synthesis kit (Invitrogen) and Mir-X miRNA First-Strand Synthesis Kit (Takara Bio), respectively. We quantified the levels of targeted mRNA or miRNA transcripts using quantitative real-time PCR in an LightCycler 480 II machine (Roche) using specific primers (forward 5′-CTCGCTT CGGCAGCACA-3′ and reverse 5′-AACGCTTCACGAATTTGCGT-3′ for U6; forward 5′-CTTGTCCTTCATTCCACCGGA-3′ and reverse 5′-TGCCGCCTGAACTTCACTCC-3′ for miR-205-5p; forward 5′-TC

CATCTTGCTCCAACACCC-3′ and reverse 5′-TCGTCTTTCCGTG CTCCAAA-3′ for pGL3; forward 5′-GAAGGTGAAGGTCGGAGT C-3′ and reverse 5′-GAAAGATGGTGATGGGATTTC-3′ for GAP DH; forward 5′-CAGATACACTTACTCGGAGTGG-3′ and reverse 5′-CCATCTTCTTCTTGTCGTTCAC-3′ for DSC2; forward 5′-TGT TAATCTCGCCTGGCGGAG-3′ and reverse 5′-GAAAGCCACGGG TGGGAACT-3′ for DSC2 3′ UTR; Shanghai Sangon Biological). We analyzed the data using $2^{-\Delta\Delta Ct}$.

Western blot
We analyzed the relative levels of interesting protein to the control α-tubulin expression using western blotting.[62] The antibodies used included anti-DSC2 (60239-1-Ig; Proteintech), anti-phospho-EFGR-Y845 (AP0023; ABclonal), anti-EGFR (A11577; ABclonal), anti-phospho-ERK1-T202/Y204 + ERK2-T185/Y187 (AP0472; AB-clonal), anti-ERK1/ERK2 (A10613; ABclonal), anti-MMP2 (66366-1-Ig; Proteintech), anti-MMP9 (10375-2-AP; Proteintech), and anti-α-tubulin (AF0001; Beyotime). We quantified the data by densitometric scanning using ImageJ software.

Statistical analysis
Data are expressed as mean ± SD and were analyzed by Student's *t* test and Pearson correlation coefficients using GraphPad Prism 7.0. A p value of < 0.05 was considered to indicate statistical significance.

SUPPLEMENTAL INFORMATION
Supplemental information can be found online at https://doi.org/10.1016/j.omto.2022.02.008.

AUTHOR CONTRIBUTIONS
H.W., Q.L., Y.Z., J.L., N.W., Y.H., Y.T. (Yanyan Tang), M.S., X.L., and W.Y. contributed to the conception of the study. W.Y., S.T., L.Y., L.O., and L.X. performed the experiments. W.Y., S.T., X.C., R.Y., Y.Y., L.H., Z.H., Y.T. (Yi Tao), L.L., and Y.J. contributed significantly to analysis and manuscript preparation.

DECLARATION OF INTERESTS
The authors declare no competing interests.

REFERENCES

1. Chen, Y.P., Chan, A.T.C., Le, Q.T., Blanchard, P., Sun, Y., and Ma, J. (2019). Nasopharyngeal carcinoma. Lancet *394*, 64–80. https://doi.org/10.1016/S0140-6736(19)30956-0.

2. You, R., Liu, Y.P., Huang, P.Y., Zou, X., Sun, R., He, Y.X., Wu, Y.S., Shen, G.P., Zhang, H.D., Duan, C.Y., et al. (2020). Efficacy and safety of locoregional radiotherapy with chemotherapy vs chemotherapy alone in de novo metastatic nasopharyngeal carcinoma: a multicenter phase 3 randomized clinical trial. JAMA Oncol. *6*, 1345–1352. https://doi.org/10.1001/jamaoncol.2020.1808.

3. Singhal, M., and Augustin, H.G. (2020). Beyond angiogenesis: exploiting angiocrine factors to restrict tumor progression and metastasis. Cancer Res. *80*, 659–662. https://doi.org/10.1158/0008-5472.CAN-19-3351.

4. Fu, L.Q., Du, W.L., Cai, M.H., Yao, J.Y., Zhao, Y.Y., and Mou, X.Z. (2020). The roles of tumor-associated macrophages in tumor angiogenesis and metastasis. Cell. Immunol. *353*, 104119. https://doi.org/10.1016/j.cellimm.2020.104119.

5. Piawah, S., and Venook, A.P. (2019). Targeted therapy for colorectal cancer metastases: a review of current methods of molecularly targeted therapy and the use of tumor biomarkers in the treatment of metastatic colorectal cancer. Cancer *125*, 4139–4147. https://doi.org/10.1002/cncr.32163.

6. Annese, T., Tamma, R., De Giorgis, M., and Ribatti, D. (2020). microRNAs biogenesis, functions and role in tumor angiogenesis. Front. Oncol. *10*, 581007. https://doi.org/10.3389/fonc.2020.581007.

7. McGeary, S.E., Lin, K.S., Shi, C.Y., Pham, T.M., Bisaria, N., Kelley, G.M., and Bartel, D.P. (2019). The biochemical basis of microRNA targeting efficacy. Science *366*. https://doi.org/10.1126/science.aav1741.

8. Santovito, D., Egea, V., Bidzhekov, K., Natarelli, L., Mourao, A., Blanchet, X., Wichapong, K., Aslani, M., Brunssen, C., Horckmans, M., et al. (2020). Noncanonical inhibition of caspase-3 by a nuclear microRNA confers endothelial protection by autophagy in atherosclerosis. Sci. Transl. Med. *12*, eaaz2294. https://doi.org/10.1126/scitranslmed.aaz2294.

9. Wang, T.Y., Wang, W., Li, F.F., Chen, Y.C., Jiang, D., Chen, Y.D., Yang, H., Liu, L., Lu, M., Sun, J.S., et al. (2020). Maggot excretions/secretions promote diabetic wound angiogenesis via miR18a/19a - TSP-1 axis. Diabetes Res. Clin. Pract. *165*, 108140. https://doi.org/10.1016/j.diabres.2020.108140.

10. Mitra, R., Adams, C.M., Jiang, W., Greenawalt, E., and Eischen, C.M. (2020). Pan-cancer analysis reveals cooperativity of both strands of microRNA that regulate tumorigenesis and patient survival. Nat. Commun. *11*, 968. https://doi.org/10.1038/s41467-020-14713-2.

11. Chen, X., Yang, F., Zhang, T., Wang, W., Xi, W., Li, Y., Zhang, D., Huo, Y., Zhang, J., Yang, A., and Wang, T. (2019). MiR-9 promotes tumorigenesis and angiogenesis and is activated by MYC and OCT4 in human glioma. J. Exp. Clin. Cancer Res. *38*, 99. https://doi.org/10.1186/s13046-019-1078-2.

12. Yan, S., Wang, H., Chen, X., Liang, C., Shang, W., Wang, L., Li, J., and Xu, D. (2020). MiR-182-5p inhibits colon cancer tumorigenesis, angiogenesis, and lymphangiogenesis by directly downregulating VEGF-C. Cancer Lett. *488*, 18–26. https://doi.org/10.1016/j.canlet.2020.04.021.

13. O'Brien, K., Breyne, K., Ughetto, S., Laurent, L.C., and Breakefield, X.O. (2020). RNA delivery by extracellular vesicles in mammalian cells and its applications. Nat. Rev. Mol. Cell Biol. *21*, 585–606. https://doi.org/10.1038/s41580-020-0251-y.

14. Kalluri, R., and LeBleu, V.S. (2020). The biology, function, and biomedical applications of exosomes. Science *367*, eaau6977. https://doi.org/10.1126/science.aau6977.

15. Zhang, X., Zhang, H., Gu, J., Zhang, J., Shi, H., Qian, H., Wang, D., Xu, W., Pan, J., and Santos, H.A. (2021). Engineered extracellular vesicles for cancer therapy. Adv. Mater. *33*, e2005709. https://doi.org/10.1002/adma.202005709.

16. Matarredona, E.R., and Pastor, A.M. (2019). Extracellular vesicle-mediated communication between the glioblastoma and its microenvironment. Cells *9*, 96. https://doi.org/10.3390/cells9010096.

17. Zhang, D.X., Vu, L.T., Ismail, N.N., Le, M.T.N., and Grimson, A. (2021). Landscape of extracellular vesicles in the tumour microenvironment: interactions with stromal cells and with non-cell components, and impacts on metabolic reprogramming, horizontal transfer of neoplastic traits, and the emergence of therapeutic resistance. Semin. Cancer Biol. *74*, 24–44. https://doi.org/10.1016/j.semcancer.2021.01.007.

18. Feng, Y., Wang, L., Wang, T., Li, Y., Xun, Q., Zhang, R., Liu, L., Li, L., Wang, W., Tian, Y., et al. (2021). Tumor cell-secreted exosomal miR-22-3p inhibits transgelin and induces vascular abnormalization to promote tumor budding. Mol. Ther. 29, 2151–2166. https://doi.org/10.1016/j.ymthe.2021.02.009.

19. Zeng, Z., Li, Y., Pan, Y., Lan, X., Song, F., Sun, J., Zhou, K., Liu, X., Ren, X., Wang, F., et al. (2018). Cancer-derived exosomal miR-25-3p promotes pre-metastatic niche formation by inducing vascular permeability and angiogenesis. Nat. Commun. 9, 5395. https://doi.org/10.1038/s41467-018-07810-w.

20. Bao, L., You, B., Shi, S., Shan, Y., Zhang, Q., Yue, H., Zhang, J., Zhang, W., Shi, Y., Liu, Y., et al. (2018). Metastasis-associated miR-23a from nasopharyngeal carcinoma-derived exosomes mediates angiogenesis by repressing a novel target gene TSGA10. Oncogene 37, 2873–2889. https://doi.org/10.1038/s41388-018-0183-6.

21. Lu, J., Liu, Q.H., Wang, F., Tan, J.J., Deng, Y.Q., Peng, X.H., Liu, X., Zhang, B., Xu, X., and Li, X.P. (2018). Exosomal miR-9 inhibits angiogenesis by targeting MDK and regulating PDK/AKT pathway in nasopharyngeal carcinoma. J. Exp. Clin. Cancer Res. 37, 147. https://doi.org/10.1186/s13046-018-0814-3.

22. Ge, X., Niture, S., Lin, M., Cagle, P., Li, P.A., and Kumar, D. (2021). MicroRNA-205-5p inhibits skin cancer cell proliferation and increase drug sensitivity by targeting TNFAIP8. Sci. Rep. 11, 5660. https://doi.org/10.1038/s41598-021-85097-6.

23. Lin, L.F., Li, Y.T., Han, H., and Lin, S.G. (2021). MicroRNA-205-5p targets the HOXD9-Snail1 axis to inhibit triple negative breast cancer cell proliferation and chemoresistance. Aging (Albany NY) 13, 3945–3956. https://doi.org/10.18632/aging.202363.

24. Zhang, Z., He, X., Xu, J., Zhang, G., Yang, Y., Ma, J., Sun, Y., Ni, H., and Wang, F. (2020). Advantages of restoring miR-205-3p expression for better prognosis of gastric cancer via prevention of epithelial-mesenchymal transition. J. Gastric Cancer 20, 212–224. https://doi.org/10.5230/jgc.2020.20.e19.

25. Yin, X., Huo, Z., Yan, S., Wang, Z., Yang, T., Wu, H., and Zhang, Z. (2021). MiR-205 inhibits sporadic vestibular schwannoma cell proliferation by targeting cyclin-dependent kinase 14. World Neurosurg. 147, e25–e31. https://doi.org/10.1016/j.wneu.2020.11.043.

26. Dong, Y., Si, J.W., Li, W.T., Liang, L., Zhao, J., Zhou, M., Li, D., and Li, T. (2015). miR-200a/miR-141 and miR-205 upregulation might be associated with hormone receptor status and prognosis in endometrial carcinomas. Int. J. Clin. Exp. Pathol. 8, 2864–2875.

27. Zhu, H., Xu, Y., Li, M., and Chen, Z. (2021). Inhibition sequence of miR-205 hinders the cell proliferation and migration of lung cancer cells by regulating PETN-mediated PI3K/AKT signal pathway. Mol. Biotechnol. 63, 587–594. https://doi.org/10.1007/s12033-021-00321-y.

28. Chu, P., Liang, A., Jiang, A., and Zong, L. (2018). miR-205 regulates the proliferation and invasion of ovarian cancer cells via suppressing PTEN/SMAD4 expression. Oncol. Lett. 15, 7571–7578. https://doi.org/10.3892/ol.2018.8313.

29. Wang, F., Lu, J., Peng, X., Wang, J., Liu, X., Chen, X., Jiang, Y., Li, X., and Zhang, B. (2016). Integrated analysis of microRNA regulatory network in nasopharyngeal carcinoma with deep sequencing. J. Exp. Clin. Cancer Res. 35, 17. https://doi.org/10.1186/s13046-016-0292-4.

30. Niu, Z., Wang, F., Lv, S., Lv, Y., Liu, M., Fu, L., Yao, Y., Wang, L., Lin, W., and Yuan, F. (2021). HNRNPU-AS1 regulates cell proliferation and apoptosis via the MicroRNA 205-5p/AXIN2 Axis and Wnt/beta-catenin signaling pathway in cervical cancer. Mol. Cell Biol. 41, e0011521. https://doi.org/10.1128/MCB.00115-21.

31. Zhang, P., Lu, X., Shi, Z., Li, X., Zhang, Y., Zhao, S., and Liu, H. (2019). miR-205-5p regulates epithelial-mesenchymal transition by targeting PTEN via PI3K/AKT signaling pathway in cisplatin-resistant nasopharyngeal carcinoma cells. Gene 710, 103–113. https://doi.org/10.1016/j.gene.2019.05.058.

32. Wang, M., Yu, F., Ding, H., Wang, Y., Li, P., and Wang, K. (2019). Emerging function and clinical values of exosomal MicroRNAs in cancer. Mol. Ther. Nucleic Acids 16, 791–804. https://doi.org/10.1016/j.omtn.2019.04.027.

33. Zhou, C.F., Ma, J., Huang, L., Yi, H.Y., Zhang, Y.M., Wu, X.G., Yan, R.M., Liang, L., Zhong, M., Yu, Y.H., et al. (2019). Cervical squamous cell carcinoma-secreted exosomal miR-221-3p promotes lymphangiogenesis and lymphatic metastasis by targeting VASH1. Oncogene 38, 1256–1268. https://doi.org/10.1038/s41388-018-0511-x.

34. Fang, W.K., Liao, L.D., Li, L.Y., Xie, Y.M., Xu, X.E., Zhao, W.J., Wu, J.Y., Zhu, M.X., Wu, Z.Y., Du, Z.P., et al. (2013). Down-regulated desmocollin-2 promotes cell aggressiveness through redistributing adherens junctions and activating beta-catenin signalling in oesophageal squamous cell carcinoma. J. Pathol. 231, 257–270. https://doi.org/10.1002/path.4236.

35. Wang, M., Zhao, Y., Yu, Z.Y., Zhang, R.D., Li, S.A., Zhang, P., Shan, T.K., Liu, X.Y., Wang, Z.M., Zhao, P.C., and Sun, H.W. (2020). Glioma exosomal microRNA-148a-3p promotes tumor angiogenesis through activating the EGFR/MAPK signaling pathway via inhibiting ERRFI1. Cancer Cell Int. 20, 518. https://doi.org/10.1186/s12935-020-01566-4.

36. Chen, L., Lin, G., Chen, K., Liang, R., Wan, F., Zhang, C., Tian, G., and Zhu, X. (2020). VEGF promotes migration and invasion by regulating EMT and MMPs in nasopharyngeal carcinoma. J. Cancer 11, 7291–7301. https://doi.org/10.7150/jca.46429.

37. Yang, Y., Ma, L., Xu, Y., Liu, Y., Li, W., Cai, J., and Zhang, Y. (2020). Enalapril overcomes chemoresistance and potentiates antitumor efficacy of 5-FU in colorectal cancer by suppressing proliferation, angiogenesis, and NF-kappaB/STAT3-regulated proteins. Cell Death Dis. 11, 477. https://doi.org/10.1038/s41419-020-2675-x.

38. Cai, H.P., Wang, J., Xi, S.Y., Ni, X.R., Chen, Y.S., Yu, Y.J., Cen, Z.W., Yu, Z.H., Chen, F.R., Guo, C.C., et al. (2019). Tenascin-cmediated vasculogenic mimicry formation via regulation of MMP2/MMP9 in glioma. Cell Death Dis 10, 879. https://doi.org/10.1038/s41419-019-2102-3.

39. Zhou, Q., Huang, T., Jiang, Z., Ge, C., Chen, X., Zhang, L., Zhao, F., Zhu, M., Chen, T., Cui, Y., et al. (2020). Upregulation of SNX5 predicts poor prognosis and promotes hepatocellular carcinoma progression by modulating the EGFR-ERK1/2 signaling pathway. Oncogene 39, 2140–2155. https://doi.org/10.1038/s41388-019-1131-9.

40. Zheng, S., Lu, Z., Liu, C., Wang, X., Jin, R., Mao, S., Huang, J., Lei, Y., Zhang, C., Sun, N., and He, J. (2019). The TGFbeta-induced long non-coding RNA TBULC promotes the invasion and migration of non-small cell lung cancer cells and indicates poor prognosis. Front. Oncol. 9, 1340. https://doi.org/10.3389/fonc.2019.01340.

41. He, S.W., Xu, C., Li, Y.Q., Li, Y.Q., Zhao, Y., Zhang, P.P., Lei, Y., Liang, Y.L., Li, J.Y., Li, Q., et al. (2020). AR-induced long non-coding RNA LINC01503 facilitates proliferation and metastasis via the SFPQ-FOSL1 axis in nasopharyngeal carcinoma. Oncogene 39, 5616–5632. https://doi.org/10.1038/s41388-020-01388-8.

42. Olejarz, W., Kubiak-Tomaszewska, G., Chrzanowska, A., and Lorenc, T. (2020). Exosomes in angiogenesis and anti-angiogenic therapy in cancers. Int. J. Mol. Sci. 21, 5840. https://doi.org/10.3390/ijms21165840.

43. Mao, S., Lu, Z., Zheng, S., Zhang, H., Zhang, G., Wang, F., Huang, J., Lei, Y., Wang, X., Liu, C., et al. (2020). Exosomal miR-141 promotes tumor angiogenesis via KLF12 in small cell lung cancer. J. Exp. Clin. Cancer Res. 39, 193. https://doi.org/10.1186/s13046-020-01680-1.

44. Kim, D.H., Park, S., Kim, H., Choi, Y.J., Kim, S.Y., Sung, K.J., Sung, Y.H., Choi, C.M., Yun, M., Yi, Y.S., et al. (2020). Tumor-derived exosomal miR-619-5p promotes tumor angiogenesis and metastasis through the inhibition of RCAN1.4. Cancer Lett. 475, 2–13. https://doi.org/10.1016/j.canlet.2020.01.023.

45. He, L., Zhu, W., Chen, Q., Yuan, Y., Wang, Y., Wang, J., and Wu, X. (2019). Ovarian cancer cell-secreted exosomal miR-205 promotes metastasis by inducing angiogenesis. Theranostics 9, 8206–8220. https://doi.org/10.7150/thno.37455.

46. Jurcic, V., Kukovic, J., and Zidar, N. (2015). Expression of desmosomal proteins in acantholytic squamous cell carcinoma of the skin. Histol. Histopathol. 30, 945–953. https://doi.org/10.14670/HH-11-599.

47. Chen, J., O'Shea, C., Fitzpatrick, J.E., Koster, M.I., and Koch, P.J. (2012). Loss of Desmocollin 3 in skin tumor development and progression. Mol. Carcinog. 51, 535–545. https://doi.org/10.1002/mc.20818.

48. Cui, T., Yang, L., Ma, Y., Petersen, I., and Chen, Y. (2019). Desmocollin 3 has a tumor suppressive activity through inhibition of AKT pathway in colorectal cancer. Exp. Cell Res. 378, 124–130. https://doi.org/10.1016/j.yexcr.2019.03.015.

49. Kamekura, R., Kolegraff, K.N., Nava, P., Hilgarth, R.S., Feng, M., Parkos, C.A., and Nusrat, A. (2014). Loss of the desmosomal cadherin desmoglein-2 suppresses colon cancer cell proliferation through EGFR signaling. Oncogene 33, 4531–4536. https://doi.org/10.1038/onc.2013.442.

50. Kolegraff, K., Nava, P., Helms, M.N., Parkos, C.A., and Nusrat, A. (2011). Loss of desmocollin-2 confers a tumorigenic phenotype to colonic epithelial cells through activation of Akt/beta-catenin signaling. Mol. Biol. Cell 22, 1121–1134. https://doi.org/10.1091/mbc.E10-10-0845.

51. Li, F., Zhao, X., Sun, R., Ou, J., Huang, J., Yang, N., Xu, T., Li, J., He, X., Li, C., et al. (2020). EGFR-rich extracellular vesicles derived from highly metastatic nasopharyngeal carcinoma cells accelerate tumour metastasis through PI3K/AKT pathway-suppressed ROS. J. Extracell Vesicles 10, e12003. https://doi.org/10.1002/jev2.12003.

52. Qin, H., Liu, X., Li, F., Miao, L., Li, T., Xu, B., An, X., Muth, A., Thompson, P.R., Coonrod, S.A., and Zhang, X. (2017). PAD1 promotes epithelial-mesenchymal transition and metastasis in triple-negative breast cancer cells by regulating MEK1-ERK1/2-MMP2 signaling. Cancer Lett. 409, 30–41. https://doi.org/10.1016/j.canlet.2017.08.019.

53. Chen, C.M., Hsieh, S.C., Lin, C.L., Lin, Y.S., Tsai, J.P., and Hsieh, Y.H. (2017). Alpha-mangostin suppresses the metastasis of human renal carcinoma cells by targeting MEK/ERK expression and MMP-9 transcription activity. Cell. Physiol. Biochem. 44, 1460–1470. https://doi.org/10.1159/000485582.

54. Kang, A.R., Cho, J.H., Lee, N.G., Song, J.Y., Hwang, S.G., Lee, D.H., Um, H.D., and Park, J.K. (2020). RIP1 is a novel component of gamma-ionizing radiation-induced invasion of non-small cell lung cancer cells. Int. J. Mol. Sci. 21, 4584. https://doi.org/10.3390/ijms21134584.

55. Lin, L., Cheng, K., He, Z., Lin, Q., Huang, Y., Chen, C., Xie, Z., Chen, L., and Liang, Z. (2019). A polysaccharide from Hedyotis diffusa interrupts metastatic potential of lung adenocarcinoma A549 cells by inhibiting EMT via EGFR/Akt/ERK signaling pathways. Int. J. Biol. Macromol. 129, 706–714. https://doi.org/10.1016/j.ijbiomac.2019.02.040.

56. Elbaz, M., Nasser, M.W., Ravi, J., Wani, N.A., Ahirwar, D.K., Zhao, H., Oghumu, S., Satoskar, A.R., Shilo, K., Carson, W.E., 3rd, and Ganju, R.K. (2015). Modulation of the tumor microenvironment and inhibition of EGF/EGFR pathway: novel anti-tumor mechanisms of Cannabidiol in breast cancer. Mol. Oncol. 9, 906–919. https://doi.org/10.1016/j.molonc.2014.12.010.

57. Yarden, Y., and Shilo, B.Z. (2007). SnapShot: EGFR signaling pathway. Cell 131, 1018. https://doi.org/10.1016/j.cell.2007.11.013.

58. Cocozza, F., Grisard, E., Martin-Jaular, L., Mathieu, M., and Thery, C. (2020). SnapShot: extracellular vesicles. Cell 182, 262–262 e261. https://doi.org/10.1016/j.cell.2020.04.054.

59. Zhu, L., Sun, H.T., Wang, S., Huang, S.L., Zheng, Y., Wang, C.Q., Hu, B.Y., Qin, W., Zou, T.T., Fu, Y., et al. (2020). Isolation and characterization of exosomes for cancer research. J. Hematol. Oncol. 13, 152. https://doi.org/10.1186/s13045-020-00987-y.

60. Makarova, J., Turchinovich, A., Shkurnikov, M., and Tonevitsky, A. (2021). Extracellular miRNAs and cell-cell communication: problems and prospects. Trends Biochem. Sci. 46, 640–651. https://doi.org/10.1016/j.tibs.2021.01.007.

61. Xia, L., Lin, J., Su, J., Oyang, L., Wang, H., Tan, S., Tang, Y., Chen, X., Liu, W., Luo, X., et al. (2019). Diallyl disulfide inhibits colon cancer metastasis by suppressing Rac1-mediated epithelial-mesenchymal transition. Onco Targets Ther. 12, 5713–5728. https://doi.org/10.2147/OTT.S208738.

62. Tan, S., Yi, P., Wang, H., Xia, L., Han, Y., Wang, H., Zeng, B., Tang, L., Pan, Q., Tian, Y., et al. (2020). RAC1 involves in the radioresistance by mediating epithelial-mesenchymal transition in lung cancer. Front. Oncol. 10, 649. https://doi.org/10.3389/fonc.2020.00649.

63. Liu, H.T., Ma, R.R., Lv, B.B., Zhang, H., Shi, D.B., Guo, X.Y., Zhang, G.H., and Gao, P. (2020). LncRNA-HNF1A-AS1 functions as a competing endogenous RNA to activate PI3K/AKT signalling pathway by sponging miR-30b-3p in gastric cancer. Br. J. Cancer 122, 1825–1836. https://doi.org/10.1038/s41416-020-0836-4.

Supplemental information

Exosomal miR-205-5p enhances angiogenesis

and nasopharyngeal carcinoma metastasis

by targeting *desmocollin-2*

Wenjuan Yang, Shiming Tan, Lixia Yang, Xiaohui Chen, Ruiqian Yang, Linda Oyang, Jinguan Lin, Longzheng Xia, Nayiyuan Wu, Yaqian Han, Yanyan Tang, Min Su, Xia Luo, Yiqing Yang, Lisheng Huang, Zifan Hu, Yi Tao, Lin Liu, Yi Jin, Hui Wang, Qianjin Liao, and Yujuan Zhou
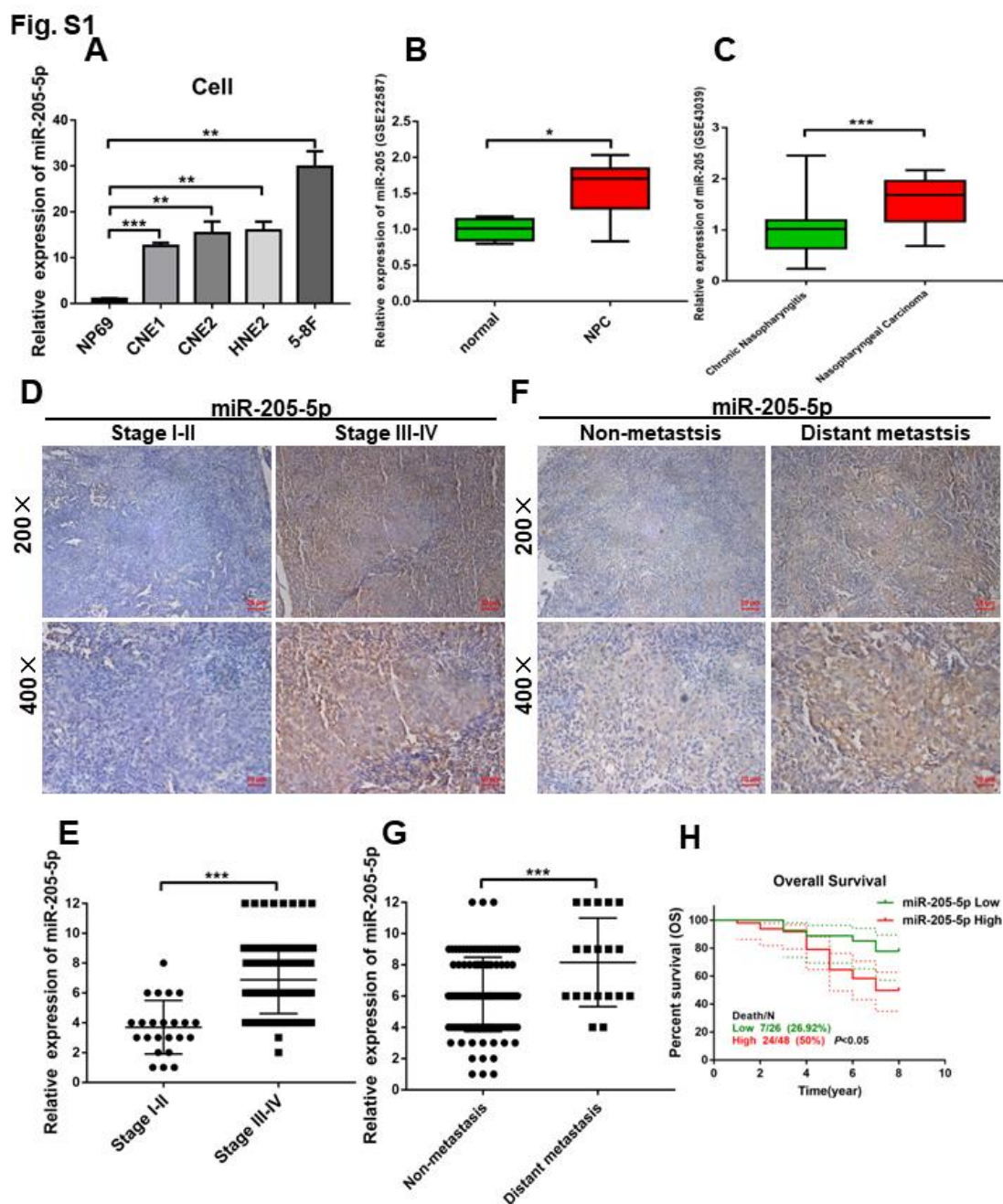
Supplementary figure legends:

Fig. S1

Figure S1. Up-regulated miR-205-5p transcripts are linked to tumor progression and worse prognosis of NPC. (A) The relative levels of miR-205-5p transcripts in the indicated cell lines, determined by qRT-PCR. **(B and C)** The levels of miR-205 transcripts in NPC (n=28) and control (n=24) tissues of the GSE22587 and GSE43039. **(D, E)** ISH analysis of miR-205-5p transcripts in stage I-II (n=23) and stage III-IV

(n=112) of NPC tissues. The scale bar in 200× images represents 50 μm. The scale bar in 400× images represents 10 μm. **(F, G)** ISH analysis of miR-205-5p transcripts in NPC (n=135) and distant metastatic NPC (n=19) tissues. The scale bar in 200× images represents 50 μm. The scale bar in 400× images represents 10 μm. **(H)** High levels miR-205-5p transcripts were associated with worse overall survival of NPC patients (n=48 for high; n=27 for low). Data are representative images (magnification x 200 and x 400) or expressed as individual values, mean ± SD or mean ± 49.6% interquartile range (IQR) from three separate experiments. * *P*<0.05, ** *P*<0.01, *** *P*<0.001.
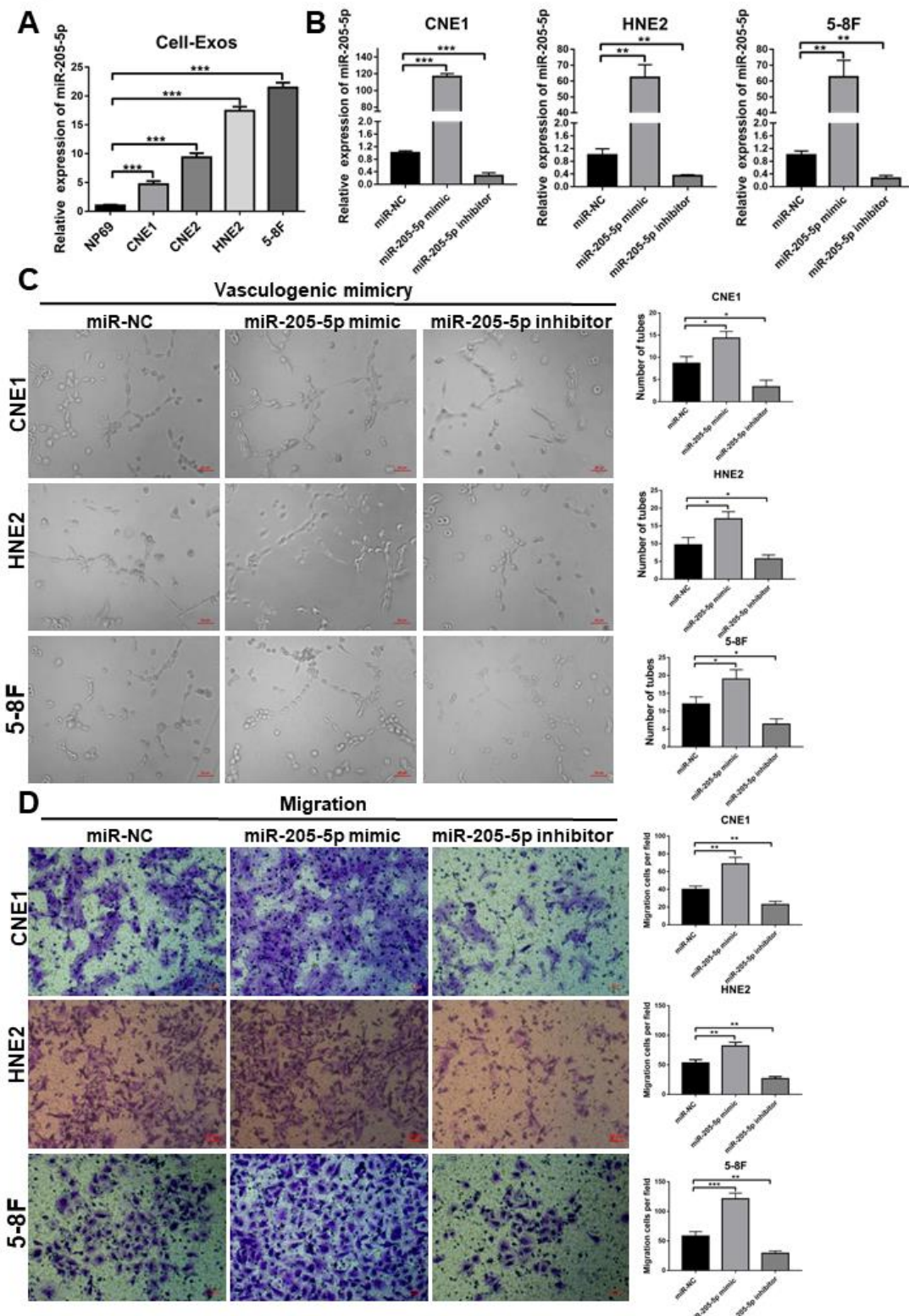
Figure S2. MiR-205-5p promotes the VM and migration of NPC cells.

(A) The relative levels of exosomal miR-205-5p in the supernatants of cultured cells, determined by qRT-PCR. **(B)** qRT-PCR verification of miR-205-5p over-expression

and silencing in NPC cells. **(C, D)** Altered miR-205-5p transcripts affected the VM, migration and invasion of the indicated NPC cells. These data indicated that miR-205-5p over-expression significantly enhanced the VM and migration of the indicated NPC cells *in vitro*. Scale bar, 20 μm. Data are representative images or expressed as mean $\pm$ SD of each group from three separate experiments. * $P<0.05$, ** $P<0.01$, *** $P<0.001$.
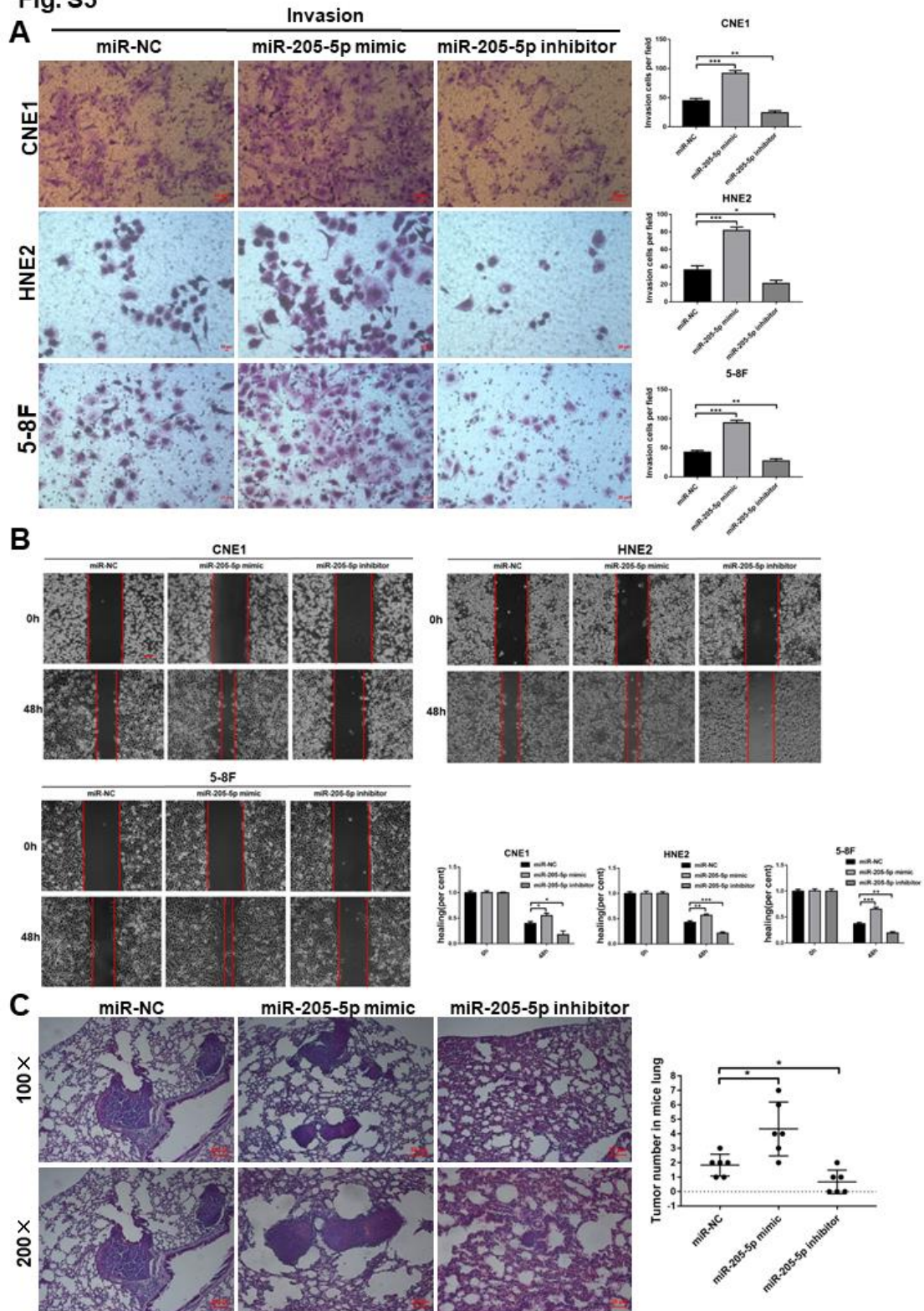
Figure S3. MiR-205-5p enhances the metastatic behaviors of NPC cells.

Altered levels of miR-205-5p transcripts modulated invasion **(A)**, wound healing **(B)** of NPC cells. The scale bar in (A) represents 20 μm. The scale bar in (B) represents

100 μm. **(C)** Altered levels of miR-205-5p transcripts affected the lung metastasis of 5-8F tumors in mice (N=6 per group)**.** These data indicated that miR-205-5p over-expression significantly enhanced the invasion and would healing of the indicated NPC cells *in vitro* and lung metastasis of 5-8F tumors *in vivo* while miR-205-5p inhibition had opposite effects. Data are representative images (magnification x 200) or expressed as mean $\pm$ SD of each group from three separate experiments. The scale bar in $100\times$ images represents 100 μm. The scale bar in $200\times$ images represents 50 μm.   * $P<0.05$, ** $P<0.01$, *** $P<0.001$.
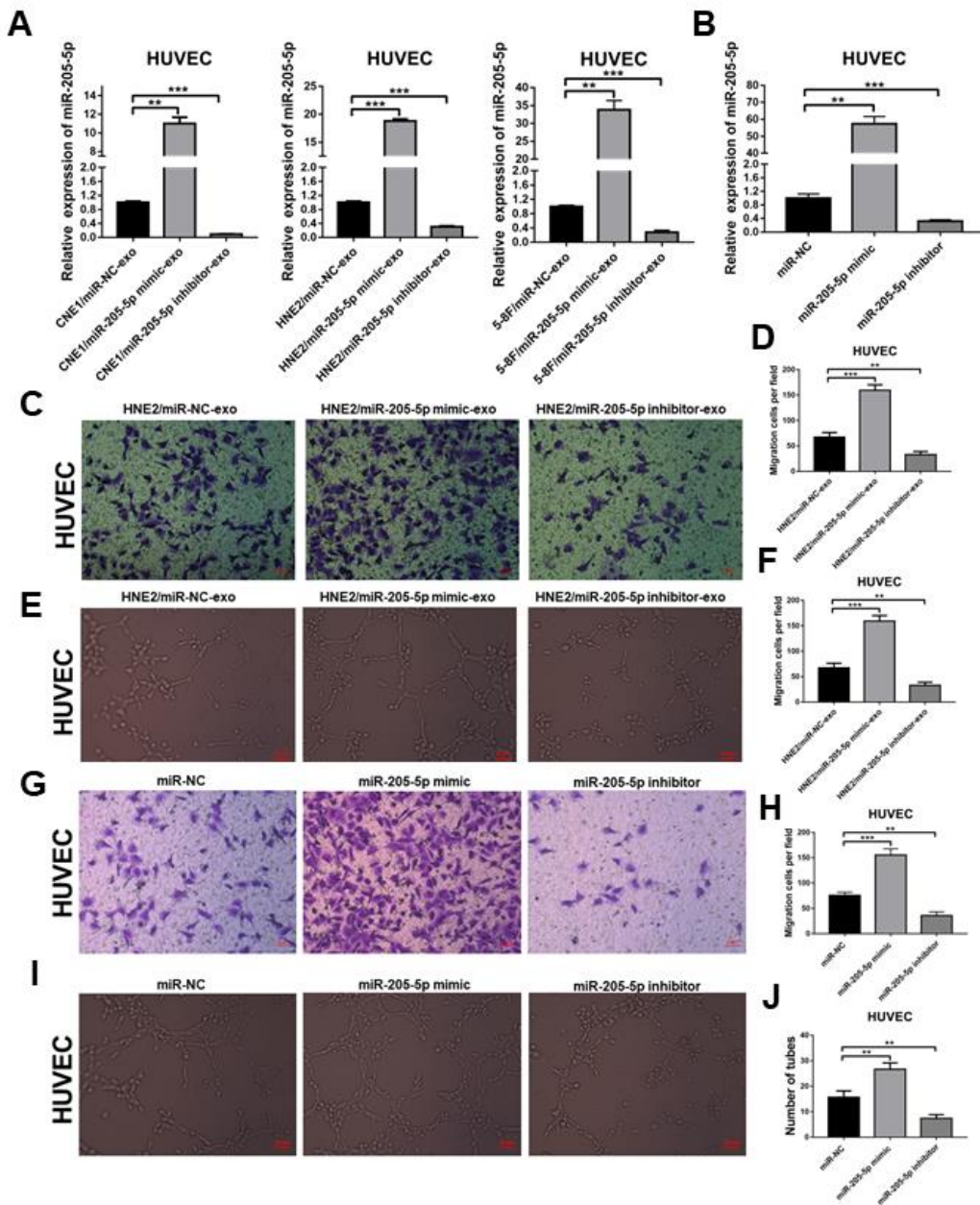
Figure S4. Exosomal miR-205-5p from different groups of NPC cells modulates the migration and tube formation of HUVECs. (A) Treatment with exosomes from the different groups of NPC cells altered the relative levels of miR-205-5p transcripts in HUVECs. **(B)** qRT-PCR verification of the efficiency of transfection with the indicated miRNA in HUVECs. **(C-F)** Treatment with exosomes from the miR-205-5p mimic-transfected HNE2 cells enhanced the migration and tube formation of HUVECs while treatment with exosomes from the miR-205-5p inhibitor-transfected HNE2 cells had opposite effects. Scale bar, 20 μm. **(G-J)** Transfection with miR-205-5p mimic significantly increased the migration and tube formation of

HUVECs while transfection with miR-205-5p inhibitor had opposite effects. Scale bar, 20 μm. Data are representative images or expressed as mean ± SD of each group from three separate experiments. ** $P<0.01$, *** $P<0.001$.
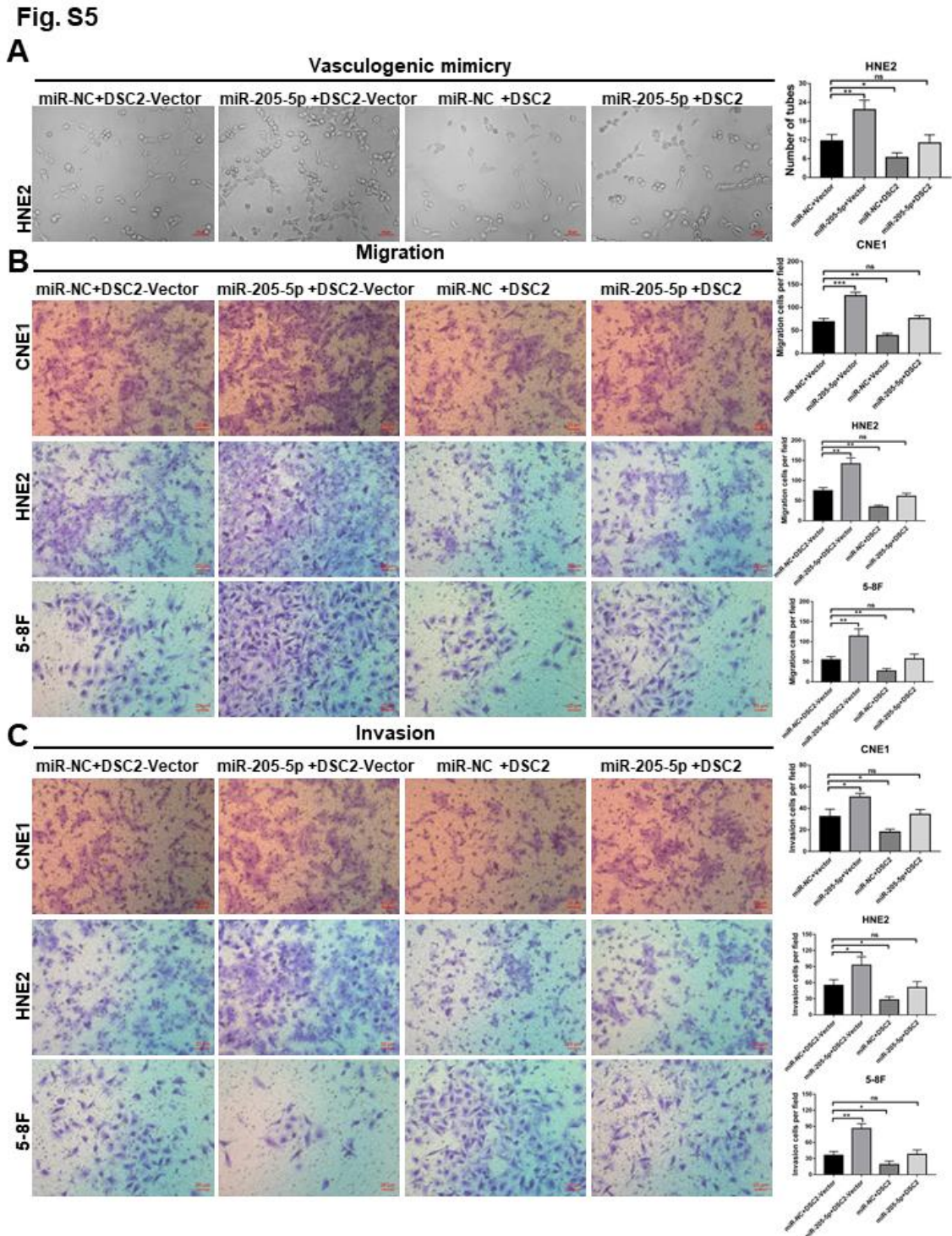

Figure S5. DSC2 over-expression abrogates the miR-205-5p-enhanced VM, migration and invasion in NPC cells.

(A-C) DSC2 over-expression abrogated the miR-205-5p-enhanced VM, migration and invasion of NPC cells. Data are representative images or expressed as mean ±SD of each group from three separate experiments. Scale bar, 20 μm. * *P*<0.05, ** *P*<0.01, *** *P*<0.001.
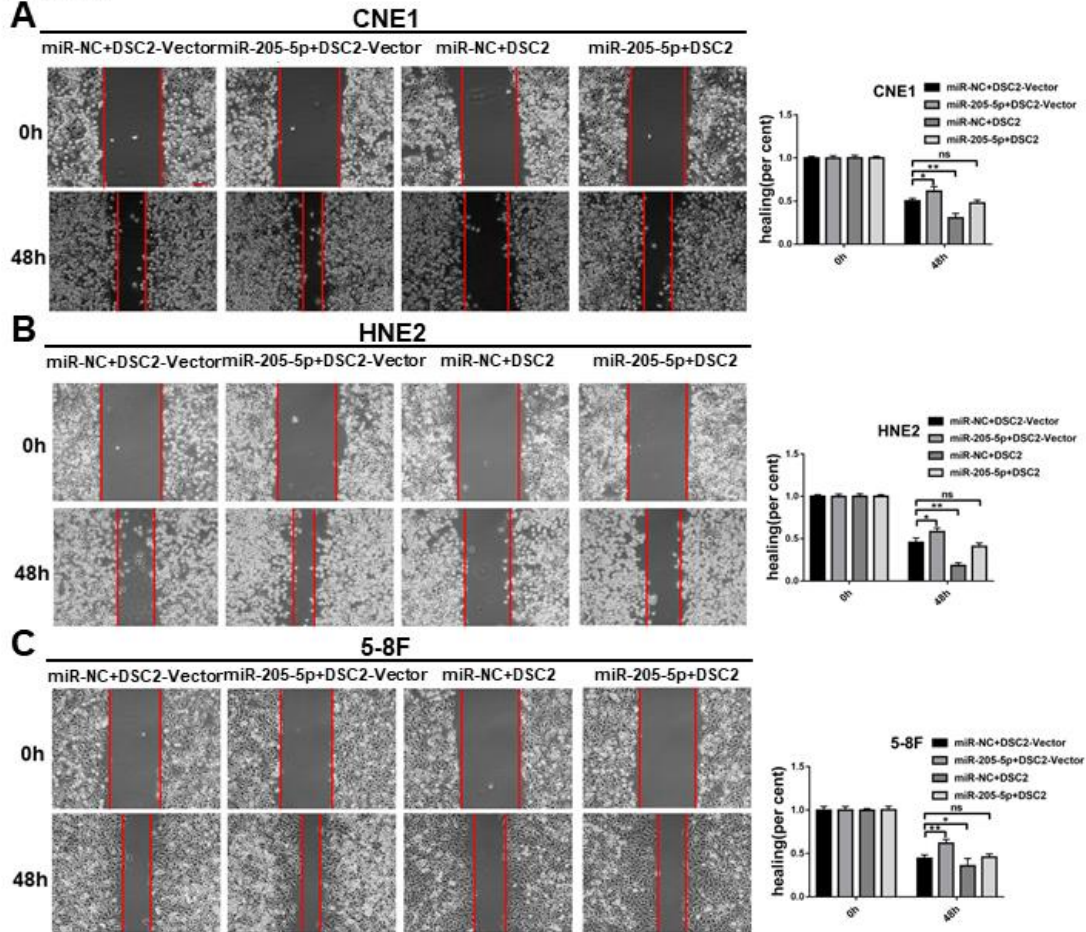

Figure S6. DSC2 over-expression abrogates the miR-205-5p-enhanced wound healing in NPC cells.

(A-C) DSC2 over-expression abrogated the miR-205-5p-enhanced wound healing in NPC cells. Data are representative images or expressed as mean ±SD of each group from three separate experiments. Scale bar, 100 μm. * *P*<0.05, ** *P*<0.01.

Fig. S7
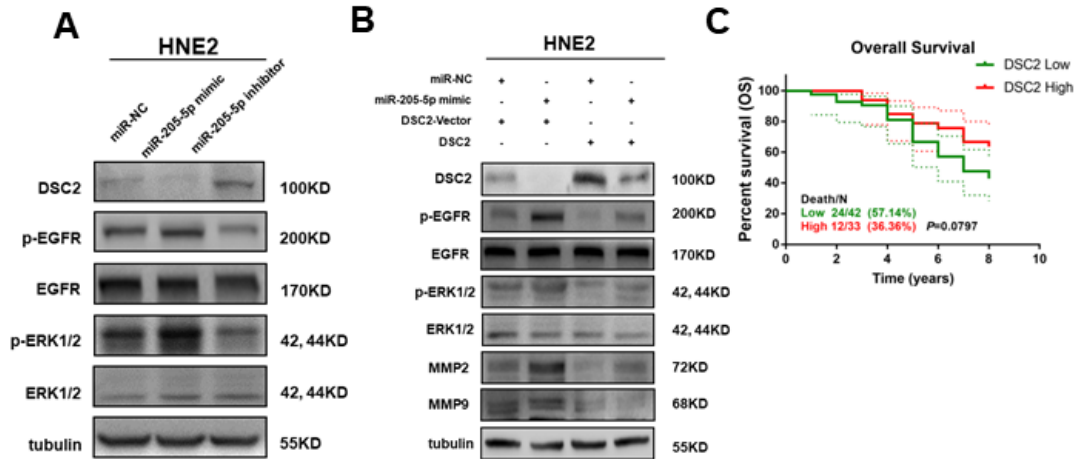
Figure S7. MiR-205-5p targets *DSC2* to enhance the EGFR/ERK signaling in HNE2 cells. (A) Western blot analysis of the relative levels of DSC2, EGFR, ERK1/2 expression and, EGFR and ERK1/2 phosphorylation in the indicated HNE2 cells. **(B)** DSC2 over-expression abrogated the miR-205-5p-enhanced EGFR/ERK1/2 activation and MMP2/MMP9 expression in HNE2 cells. **(C)** Higher levels of DSC2 expression were associated with a better overall survival of NPC patients.

Supplementary Tables:

Table S1. The association of clinical parameters with exosomal miR-205-5p in NPC patients

Items	Cases (n=88)	Exosomal miR-205-5p low	Exosomal miR-205-5p high	Chi-square	*P* value
Age (years)					
≤60	75	31	44		
				1.833	0.176
>60	13	8	5		
Gender					
Male	65	26	39		
				1.879	0.17
Female	23	13	10		
TNM stage					
T stage (T1-2)	27	19	8		
				10.71	0.001
T stage (T3-4)	61	20	41		
N stage (N0)	12	6	6		
				0.182	0.670
N stage (N1-3)	76	33	43		
Stage I, II	9	7	2		
				4.548	0.033
Stage III, IV	79	32	47		

Table S2. The association of clinical parameters with miR-205-5p in NPC

Items	Cases (n=75)	miR-205-5p Low	miR-205-5p High	Chi-square	P value
Age (years)					
≤60	63	23	40		
				0.774	0.379
>60	12	6	6		
Gender					
Male	55	21	34		
				0.02	0.886
Female	20	8	12		
TNM stage					
T stage (T1-2)	22	14	9		
				6.896	0.009
T stage (T3-4)	53	15	37		
N stage (N0)	10	5	5		
				0.625	0.429
N stage (N1-3)	65	24	41		
M stage (M0)	68	28	40		
				1.935	0.164
M stage (M1)	7	1	6		
Stage I, II	15	11	4		
				9.501	0.002
Stage III, IV	60	18	42		